Chemical Ionization

7

Learning Objectives

- Ion formation by ion–molecule reactions
- Processes of positive-ion formation other than electron ionization
- Pathways of negative-ion formation
- Softness of chemical ionization techniques
- Applications of chemical ionization mass spectrometry
- Chemical ionization processes at atmospheric pressure
- Atmospheric pressure chemical ionization
- Atmospheric pressure photoionization
- Overview of chemical ionization techniques

Mass spectrometrists have ever been searching for ionization methods softer than EI, because molecular weight determination is key for structure elucidation. *Chemical ionization* (CI) is the first of the so-called *soft ionization methods* we are going to discuss (cf. Fig. 1.4). Historically, *field ionization* (FI, Sect. 8.5) is the elder technique, and thus CI can be regarded as the second soft ionization method introduced to organic mass spectrometry. Nonetheless, CI shares some similarities with EI making its discussion next to EI convenient. CI goes back to experiments of Talrose in the early 1950s [1] and was developed to an analytically useful technique by Munson and Field in the mid-1960s [2–5]. Since then, the basic concept of CI has been extended and applied in numerous different ways, meanwhile providing experimental conditions for a wide diversity of analytical tasks [5–7].

J.H. Gross, *Mass Spectrometry*, DOI 10.1007/978-3-319-54398-7_7

7.1 Basics of Chemical Ionization

7.1.1 Formation of Ions in Positive-Ion Chemical Ionization

In chemical ionization, new ionized species are formed when gaseous molecules interact with ions, i.e., chemical ionization is based on *ion–molecule reactions* (Sect. 2.13). Chemical ionization may involve the transfer of an electron, proton, or other ions between the reactants [8], that is, between the neutral analyte M and the *reagent ions* generated from the *reagent gas* [9, 10].

CI differs from what we have encountered in mass spectrometry so far because *bimolecular processes* are used to generate analyte ions. The occurrence of bimolecular reactions requires a sufficiently large number of ion–molecule collisions during the dwell time of the reactants in the ion source. This is achieved by significantly increasing the partial pressure of the reagent gas. Assuming reasonable collision cross sections and an ion source residence time of microseconds [11], a molecule will undergo 30–70 collisions at an ion source pressure of about 2.5×10^2 Pa (2.5 mbar) [12]. The 10^3–10^4-fold excess of reagent gas also effectively shields the analyte molecules from direct ionization by primary electrons, a prerequisite to suppress competing EI of the analyte.

Let us first consider *positive-ion chemical ionization* (PICI). In PICI, there are four fundamental pathways of positive-ion formation from a neutral analyte molecule M. First, there is *proton transfer*:

$$\mathrm{M} + [\mathrm{BH}]^+ \rightarrow [\mathrm{M} + \mathrm{H}]^+ + \mathrm{B} \tag{7.1}$$

For proton transfer, the reagent ion $[BH]^+$ has to act as Brønsted acid. Proton transfer yields protonated analyte molecules, $[M+H]^+$, i.e., even-electron ions that are detected at [M+1]. Although proton transfer is generally considered to yield protonated analyte molecules, $[M+H]^+$, acidic analytes themselves may form both $[M+H]^+$ and $[M–H]^-$ ions by mutual proton exchange, a behavior exploited for *negative-ion chemical ionization* (NICI, Sect. 7.5).

Second, an analyte molecule may receive a charge by adduct formation via *electrophilic addition*:

$$\mathrm{M} + \mathrm{X}^+ \rightarrow [\mathrm{M} + \mathrm{X}]^+ \tag{7.2}$$

Electrophilic addition of X^+ occurs by attachment of the entire reagent ion to an analyte molecule if protonation of M is not feasible. For example, $[M+NH_4]^+$ ions are often formed when ammonia reagent gas is used. Thus, even-electron ions are detected at an m/z value above M, the exact position of which depends on the adduct actually formed.

Third, *anion abstraction* can occur:

$$\mathrm{M} + \mathrm{X}^+ \rightarrow [\mathrm{M} - \mathrm{A}]^+ + \mathrm{AX} \tag{7.3}$$

Hydride abstraction is a commonly occurring case of *anion abstraction*, e.g., aliphatic alcohols rather yield $[M–H]^+$ ions, $[M–1]^+$, than $[M+H]^+$ ions [13, 14]. Strong leaving groups like mesylate or tosylate may also lead to even-electron cation formation via loss of an anionic group.

The fourth pathway is *charge transfer* (CT):

$$M + X^{+\bullet} \rightarrow M^{+\bullet} + X \tag{7.4}$$

Charge transfer, also known as *charge exchange* (CE), differs from the previous three processes in that it yields molecular ions, $M^{+\bullet}$, i.e., odd-electron species. Although being positive radical ions, the products of charge transfer tend to provide notably less fragmentation than those formed upon electron ionization, because the average ion internal energy from CT is much lower than after EI. CT thus yields radical ions behaving similar to molecular ions in low-energy electron ionization (Sect. 5.6).

A sort of molecular ion?
It has been common to denote $[M+H]^+$ and $[M–H]^+$ ions as *quasi-molecular ions* because they comprise the otherwise intact analyte molecule and are detected in place of a "true" molecular ion, $M^{+\bullet}$, when soft ionization methods are employed. The term was also applied to $[M+alkali]^+$ ions created by soft ionization methods other than CI. Recent recommendations are to avoid the term *quasi-molecular ion* [9, 10]. Now, ions are addressed more specifically, e.g., $[M+H]^+$ as *protonated molecules*, $[M–H]^-$ as *deprotonated molecules*, $[M+Na]^+$ ions as *sodiated molecules*, and in general $[M+X]^+$ as *cationized molecules*.

7.1.2 Chemical Ionization Ion Sources

CI ion sources exhibit close similarity to EI ion sources (Sect. 5.1). In fact, some EI ion sources can actually be switched to CI operation in seconds, i.e., they are constructed as *EI/CI combination ion sources*. Such a change requires the EI ion source to be modified according to the needs of holding a comparatively high pressure of reagent gas (some 10^2 Pa) without allowing too much leakage into the ion source housing [15]. This is accomplished by axially inserting some inner wall, e.g., a small cylinder, into the ion volume leaving only narrow entrances and exits of the ionizing primary electrons, the sample inlets, and the exiting ion beam. The ports for the reference inlet, the gas chromatograph (GC) and the direct insertion probe (DIP) need to be tightly connected to the respective inlet system during operation, e.g., the empty DIP is inserted even when another inlet actually provides the sample flow into the ion volume. The reagent gas is introduced directly into the

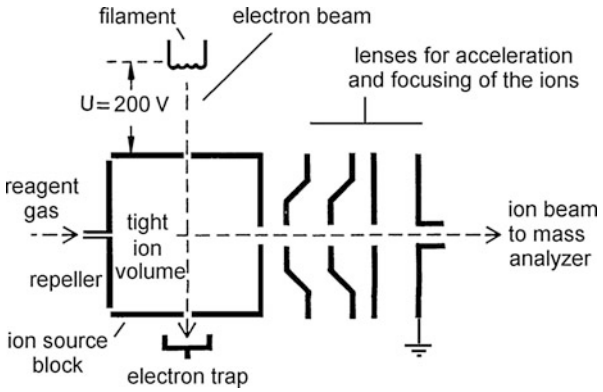

Fig. 7.1 Layout of a chemical ionization ion source (Adapted from Ref. [16] by permission. © Springer-Verlag Heidelberg, 1991)

ion volume to ensure maximum pressure inside at minimum losses to the ion source housing (Fig. 7.1). During CI operation, the pressure in the ion source housing typically rises by a factor of 20–50 (5×10^{-4}–10^{-3} Pa) as compared to the background pressure of the instrument. Thus, a sufficient pumping speed of 200 l s^{-1} or more is necessary to maintain stable operation in CI mode. The energy of the primary electrons is preferably adjusted to some 200 eV, because electrons of lower energy experience difficulties in penetrating the reagent gas.

7.1.3 Chemical Ionization Techniques and Terms

In its original implementation, chemical ionization delivered positive ions [2–5], and therefore, for many practitioners the acronym CI used without further specifications still stands for *positive-ion chemical ionization* (PICI) where the latter term should clearly be preferred. For negative ions, the term *negative-ion chemical ionization* (NICI) should be used [8]. Table 7.1 provides an overview of CI terms and acronyms. The last technique listed there, *electron capture* (EC) or *electron capture negative ionization* (ECNI) does not represent chemical ionization in the strict sense, as will be outlined later (Sect. 7.6).

7.1.4 Sensitivity of Chemical Ionization

Ionization in CI is the result of one or several competing chemical reactions. Therefore, the sensitivity (Sect. 1.6) in CI strongly depends on the conditions of the experiment. For comparison of sensitivity data, the reagent gas, its pressure, and the ion source temperature have to be stated in addition to primary electron energy and electron current. Specifications of magnetic sector instruments, for example, state a sensitivity of about 4×10^{-8} C μg^{-1} for the $[M+H]^+$ ion of methylstearate,

Table 7.1 Terms and acronyms related to chemical ionization

Polarity	Method	Acronym	Explication
Positive	Positive-ion chemical ionization (or positive chemical ionization)	PICI (or PCI)	Strictly speaking, any CI technique delivering even-electron positive analyte ions. (Sometimes used in the restricted sense of ion formation by protonation.)
	Charge transfer (or charge exchange)	CT (or CE)	Positive radical ions are formed by exchange/transfer of an electron.
Negative	Negative-ion chemical ionization (or negative chemical ionization)	NICI (or NCI)	Any CI technique delivering even-electron negative analyte ions
	Electron capture	EC (or ECNI)	Not a CI technique in the strict sense. However, ion source operation is equal to NICI

m/*z* 299, at $R = 1000$ in positive-ion CI mode with methane reagent gas. This is approximately one order of magnitude less than for EI. While the ion current that can be generated from a sample by CI tends to be lower than in EI, it is worth considering that most of this ion current is delivered by ions like $[M+H]^+$ or $[M+NH_4]^+$ that are directly related to intact molecules. Assigning the correct molecular mass is therefore easier to accomplish even in the presence of impurities.

7.2 Protonation in Chemical Ionization

7.2.1 Source of Protons

The formation of $[M+H]^+$ ions due to bimolecular processes between ions and their neutral molecular counterparts is called *autoprotonation*, a special form of *self-chemical ionization* (self-CI). Self-CI is a chemical ionization process, where the reagent ions are formed by an ionized species of the analyte itself [17]. In EI-MS, autoprotonation is an unwanted phenomenon. $[M+H]^+$ ions from autoprotonation are promoted by increasing the ion source pressure and lowering the temperature. Furthermore, the formation of $[M+H]^+$ ions is favored if the analyte is highly volatile and/or has acidic hydrogens. Thus, self-CI can cause a misinterpretation of mass spectra either by an overestimation of the number of carbon atoms from the ^{13}C isotopic peak due to exaggerated [M+1] ion abundance (Sect. 3.2) or by indicating a molecular mass which seems to be higher by 1 u than it really is (Fig. 7.6 and cf. *nitrogen rule* Sect. 6.2.7). In CI-MS with methane or ammonia reagent gas, however, the process of autoprotonation is intentionally exploited to generate the reagent ions.

Chemi-ionization
Chemi-ionization means ionization of internally excited molecules upon interaction with other neutrals by *electron detachment*. This corresponds to $M^* + X \rightarrow MX^{+\bullet} + e^-$. Chemi-ionization is different from CI in that there is no ion–molecule reaction involved (cf. Penning ionization, Sect. 2.1.3) [8, 18].

Transition from $M^{+\bullet}$ to $[M+H]^+$ The contribution of some autoprotonation causes an increase in [M+1] peak intensity that may be hard to recognize, and thus, can erroneously be interpreted as a larger number of carbon atoms than actually present (Fig. 7.2, Sect. 3.2). The appearance of the signal shifts upon transition from pure molecular ion formation to pure protonation. Conditions resulting in an intermediate situation are therefore to be avoided. Clean EI spectra require low partial pressure of the sample in the ion source while clean CI spectra demand for a correct adjustment of the reagent gas pressure in order to avoid residual EI.

7.2.2 Methane Reagent Gas Plasma

The EI mass spectrum of methane has already been discussed (Sect. 6.1). It shows peaks from all ionic species listed in Eq. 7.5. Raising the partial pressure of methane from the EI standard value of about 10^{-4} Pa to 10^2 Pa significantly alters the ion

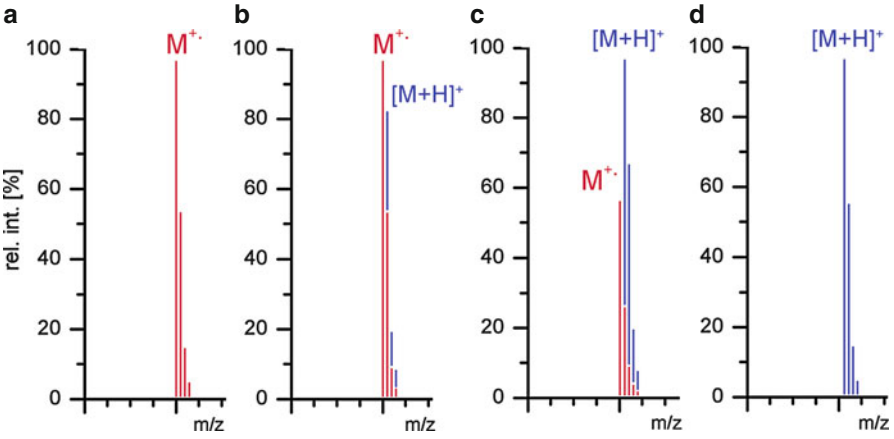

Fig. 7.2 Stepwise change of signal appearance upon transition from pure molecular ion formation (*red peak portions*) to protonated molecules (*blue peak portions*). (**a**) Pure molecular ion peak with correct isotope pattern, (**b**) some contribution of $[M+H]^+$ causes an excessively intensive [M+1] peak, (**c**) mostly $[M+H]^+$, and (**d**) pure $[M+H]^+$ ion signal with correct isotope pattern. Only pure $M^{+\bullet}$ and pure $[M+H]^+$ result in undistorted isotope patterns

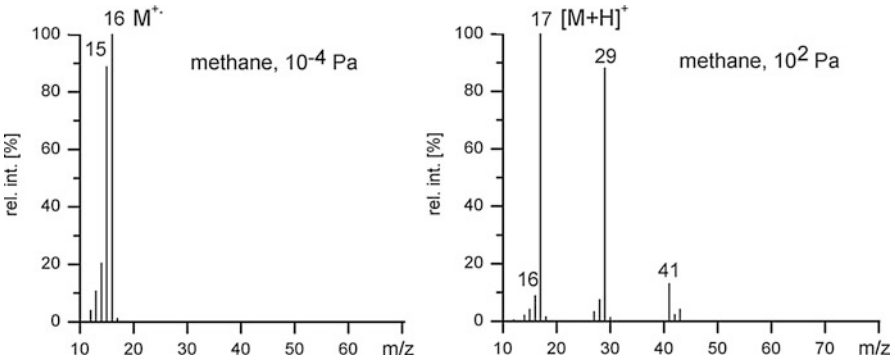

Fig. 7.3 Comparison of the methane spectrum upon electron ionization at different ion source pressures: (**a**) approx. 10^{-4} Pa, (**b**) approx. 10^{2} Pa. The latter represents the typical methane reagent gas spectrum in positive-ion CI

population [1]. The molecular ion, $CH_4^{+\bullet}$, *m*/*z* 16, almost vanishes and a new species, CH_5^+, *m*/*z* 17, is detected instead [19]. Some additional ions occur at higher mass, the most prominent being $C_2H_5^+$, *m*/*z* 29, and $C_3H_5^+$, *m*/*z* 41 (Fig. 7.3) [20, 21]. Clearly, the positive-ion CI spectrum of methane is governed by competing and consecutive bimolecular reactions in the ion source [4, 6, 12]:

$$CH_4 + e^- \rightarrow CH_4^{+\bullet},\ CH_3^+,\ CH_2^{+\bullet},\ CH^+,\ C^{+\bullet},\ H_2^{+\bullet},\ H^+ \tag{7.5}$$

$$CH_4^{+\bullet} + CH_4 \rightarrow CH_5^+ + CH_3^\bullet \tag{7.6}$$

$$CH_3^+ + CH_4 \rightarrow C_2H_7^+ \rightarrow C_2H_5^+ + H_2 \tag{7.7}$$

$$CH_2^{+\bullet} + CH_4 \rightarrow C_2H_4^{+\bullet} + H_2 \tag{7.8}$$

$$CH_2^{+\bullet} + CH_4 \rightarrow C_2H_3^+ + H_2 + H^\bullet \tag{7.9}$$

$$C_2H_3^+ + CH_4 \rightarrow C_3H_5^+ + H_2 \tag{7.10}$$

$$C_2H_5^+ + CH_4 \rightarrow C_3H_7^+ + H_2 \tag{7.11}$$

The relative abundances of the product ions change dramatically as the ion source pressure increases from EI conditions to 25 Pa. Above 100 Pa, the relative concentrations become stabilized at levels represented by the CI spectrum of methane reagent gas [4, 22]. Fortunately, in CI the ion source pressure is usually in this range of 10^2 Pa and thus in this plateau region of relative ion abundances, thereby ensuring reproducible CI conditions. The influence of the ion source temperature is more pronounced than in EI because the high collision rate rapidly effects a thermal equilibrium.

Reagent gas plasma
The simultaneous presence of free electrons, protons, and numerous ionic and radical species in the ionized reagent gas has led to its description as a *reagent gas plasma*.

7.2.3 CH_5^+ and Related Ions

The protonated methane ion, CH_5^+, represents a reactive as well as fascinating species in the methane reagent gas plasma. In 1991, its structure had been calculated as shown in Scheme 7.1 [19] and the chemical behavior of the CH_5^+ ion indeed appears to be compatible with a stable structure, involving a three-center two-electron bond associating two hydrogens and the carbon atom.

Rearrangement of this structure due to exchange between one of these hydrogens and one of the three remaining hydrogens seemingly is a fast process induced by interactions with the chemical ionization gas. Recent work indicates that all five C–H bonds are rendered equal by extremely rapid zero-point motion thereby precluding the assignment of a unique CH_5^+ ion structure [23]. For the $C_2H_7^+$ intermediate during $C_2H_5^+$ ion formation several isomerizing structures are discussed [20, 21]. In protonated fluoromethane, the conditions are quite different, promoting a weak C–F and a strong F–H bond [24].

7.2.4 Energetics of Protonation

The tendency of a (basic) molecule B to accept a proton is quantitatively described by its *proton affinity* (*PA*, Sect. 2.12). For the process of protonation we have to consider the gas phase reaction of a base, B_g, with a proton [3]:

$$B_g + H_g^+ \rightarrow [BH]_g^+ \tag{7.12}$$

Now, the proton affinity of B is defined as the negative of the corresponding heat of reaction upon formation of $[BH]_g^+$:

Scheme 7.1

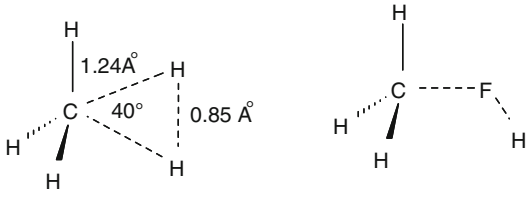

$$PA_{(B)} = -\Delta H_r{}^0 \tag{7.13}$$

The inversion of the algebraic sign of $\Delta H_r{}^0$ serves to express a more exothermal protonation in terms of a larger proton affinity of B.

To judge the chances of protonation under CI conditions, one has to compare the *PA* of the neutral analyte M with that of the complementary base B of the proton-donating reagent ion $[BH]^+$ (Brønsted acid). Protonation will occur as long as the process is exothermic, i.e., if $PA_{(B)} < PA_{(M)}$. The heat of reaction has basically to be distributed among the degrees of freedom of the $[M+H]^+$ analyte ion [14, 25]. Accordingly, the minimum internal energy of the $[M+H]^+$ ions is well approximated by:

$$E_{int(M+H)} \approx \Delta PA = PA_{(M)} - PA_{(B)} \tag{7.14}$$

Some additional thermal energy will also be contained in the $[M+H]^+$ ions. Having *PA* data at hand (Table 2.6), one can easily judge whether a reagent ion will be able to protonate the analyte of interest and how much energy will be put into the $[M+H]^+$ ion.

Influence of the substrate The $CH_5{}^+$ reagent ion is able to protonate C_2H_6 because Eq. 7.14 gives $\Delta PA = PA_{(C2H6)} - PA_{(CH4)} = 601 - 552 = 49$ kJ mol^{-1}. The product, protonated ethane, $C_2H_7{}^+$, is immediately stabilized by H_2 loss to yield $C_2H_5{}^+$ [20, 21]. In case of tetrahydrofuran, protonation to yield $[C_4H_8O+H]^+$ is more exothermic: $\Delta PA = PA_{(C4H8O)} - PA_{(CH4)} = 831 - 552 = 279$ kJ mol^{-1}, and thus, results in some more fragmentation of the $[M+H]^+$ ions.

7.2.5 Impurities of Higher *PA* than the Reagent Gas

Due to the above energetic considerations, impurities of the reagent gas having a higher *PA* than the neutral reagent gas are protonated by the reagent ion [3]. Residual water is a frequent source of contamination. Higher concentrations of water in the reagent gas may even alter its properties completely, i.e., H_3O^+ becomes the predominant species in a CH_4/H_2O mixture under CI conditions (Fig. 7.4) [26].

Impurities change reagent gas

Any analyte of suitable *PA* may be regarded as a basic impurity of the reagent gas, and thus becomes protonated in excellent yield. Heteroatoms and π-electron systems are the preferred sites of protonation. Nevertheless, the additional proton is often mobile within the ion, sometimes even accompanied by its exchange with otherwise fixed hydrogens [27, 28].

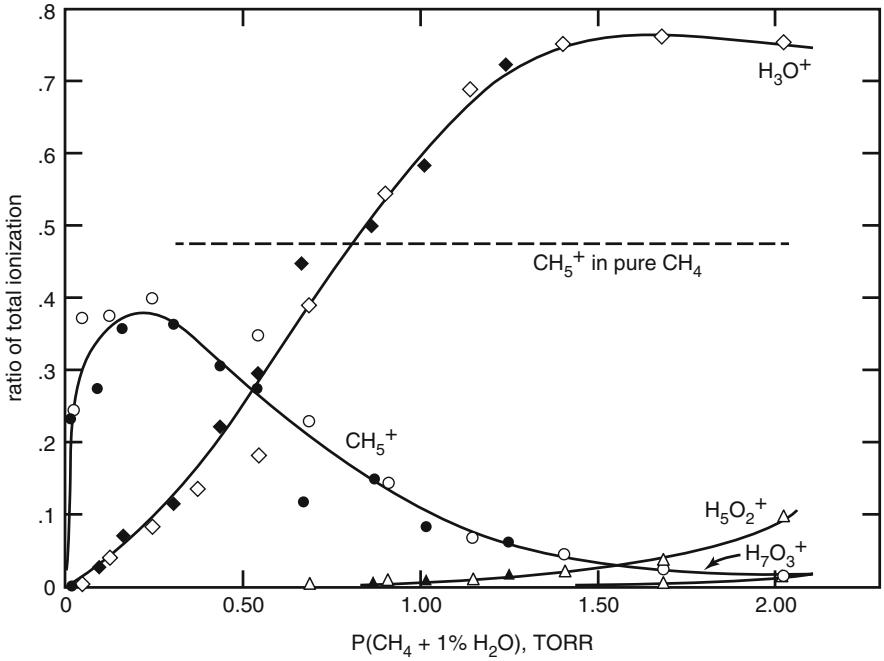

Fig. 7.4 Relative concentrations of CH_5^+ and H_3O^+ ions vs. pressure of a mixture of CH_4 (99%) and H_2O (1%). 1 Torr = 133 Pa (Reproduced from Ref. [26] by permission. © American Chemical Society, 1965)

7.2.6 Methane Reagent Gas PICI Spectra

The $[M+H]^+$ ion peak in methane reagent gas PICI spectra – generally denoted *methane-CI spectra* – is usually intense and often represents the base peak [29–31]. Although protonation in CI is generally exothermic by 1–4 eV, the degree of fragmentation of $[M+H]^+$ ions is much lower than that observed for the same analytes under 70-eV EI conditions. This is because $[M+H]^+$ ions have (*i*) a narrow internal energy distribution, and (*ii*) fast radical-induced bond cleavages are prohibited, because solely intact molecules are eliminated from these even-electron ions. Electrophilic addition fairly often gives rise to $[M+C_2H_5]^+$ and $[M+C_3H_5]^+$ adduct ions. Thus, [M+29] and [M+41] peaks are sometimes observed in addition to the expected – usually clearly dominating – [M+1] peak. Occasionally, hydride abstraction may occur instead of protonation.

Obscured hydride abstractions
Hydride abstractions are difficult to recognize. To identify a $[M–H]^+$ peak occurring instead of a $[M+H]^+$ peak it is useful to examine the mass differences between the signal in question and the products of electrophilic addition. In that case, [M+29] and [M+41] appear as if they were [M+31] and [M+43] peaks, respectively. An apparent loss of 16 u can be indicative of an $[M+H–H_2O]^+$ ion instead of an $[M+H–CH_4]^+$ ion.

PICI of methionine There is a greatly reduced fragmentation in the methane reagent gas PICI spectrum of methionine as compared to the according EI spectrum (Fig. 7.5). Only small stable molecules such as NH_3, HCOOH, and MeSH are eliminated from the $[M+H]^+$ ion, *m*/*z* 150, which yields the base peak. In addition, the PICI spectrum perfectly reveals the isotopic pattern that indicates the presence of sulfur. The horizontal line (Fig. 7.5b) means that this range was not acquired in the PICI spectrum as to keep the spectrum free from reagent ion signals. The spectra were, however, plotted on the same *m*/*z* scales to simplify the comparison.

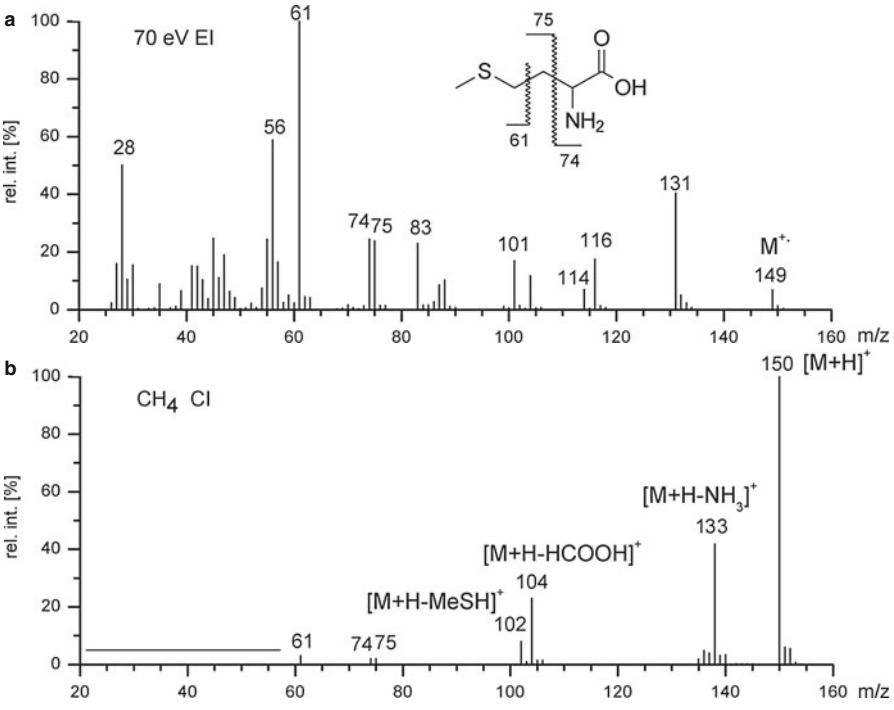

Fig. 7.5 Comparison of (**a**) 70-eV EI spectrum and (**b**) methane reagent gas PICI spectrum of the amino acid methionine

Low-mass range in CI
Resulting from the large excess of reagent gas, its spectrum often is of higher intensity than that of the analyte. Therefore, CI spectra are usually acquired starting above the *m*/*z* range occupied by reagent ions, e.g., above *m*/*z* 50 for methane or above *m*/*z* 70 for isobutane. Background subtraction can alternatively be applied to remove these peaks, but this approach suffers from variations in the reagent ion abundances upon admission of the analyte.

7.2.7 Other Reagent Gases in PICI

As pointed out, the value of ΔPA determines whether a particular analyte can be protonated by a certain reactant ion and how exothermic the protonation will be. Considering other reagent gases than methane therefore allows some tuning of the PICI conditions. The employed reagent gases and ions are chiefly:

- hydrogen and hydrogen-containing mixtures [14, 25, 32],
- isobutane [33–37],
- ammonia [34, 38–44],
- dimethylether [45],
- diisopropylether [46],
- acetone [13],
- acetaldehyde [13],
- benzene [47],
- iodomethane [48],
- nitrous oxide [39, 49, 50], and
- transition metal ions like Cu^+ [51] and Fe^+ [52].

Among these, methane, isobutane, and ammonia are the by far most common reagent gases in PICI (Table 7.2). Nitrous oxide and transition metal ions are

Table 7.2 Common PICI reagent gases (chiefly protonating)

Reagent gas	Reagent ions	Neutral from reagent ions	*PA* of neutral product [kJ mol^{-1}]	Analyte ions and relative analyte ion masses
H_2	H_3^+	H_2	424	$[M+H]^+$, $[M-H]^+$ [M+1], [M–1]
CH_4	CH_5^+ ($C_2H_5^+$ and $C_3H_5^+$)	CH_4	552	$[M+H]^+$, also $[M+C_2H_5]^+$ and $[M+C_3H_5]^+$ [M+1], [M+29], [M+41]
i-C_4H_{10}	*t*-$C_4H_9^+$	*i*-C_4H_8	820	$[M+H]^+$, also $[M+C_4H_9]^+$, (eventually $[M+C_3H_3]^+$, $[M+C_3H_5]^+$ and $[M+C_3H_7]^+$), [M+1], [M+57]
NH_3	NH_4^+	NH_3	854	$[M+H]^+$, $[M+NH_4]^+$, [M+1], [M+18]

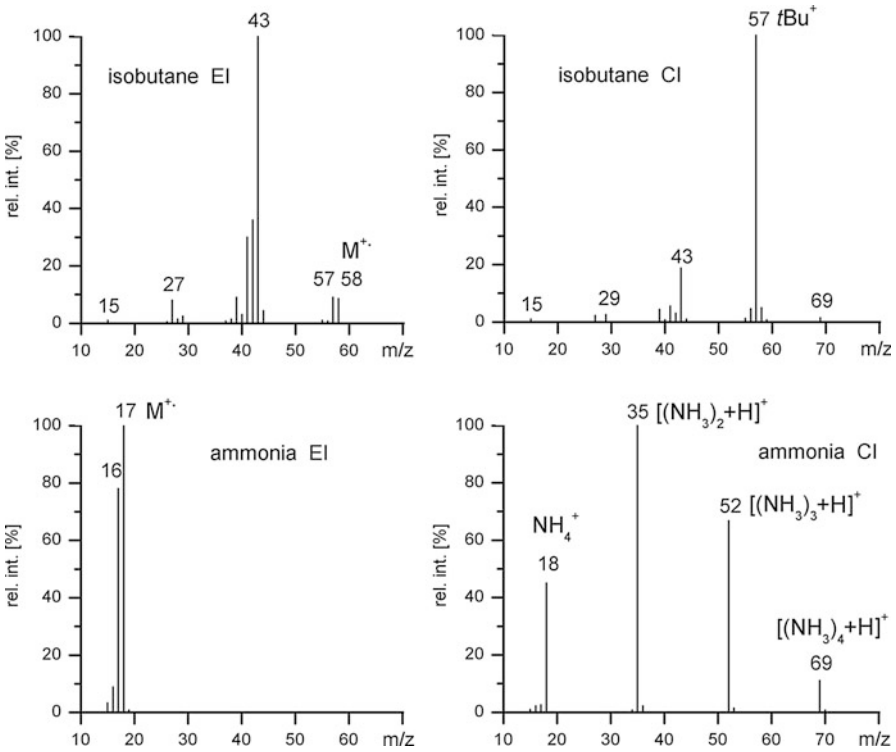

Fig. 7.6 Standard EI vs. positive-ion CI spectra of isobutane (*upper*) and ammonia (*lower part*). Ammonia forms abundant $[(NH_3)_n+H]^+$ cluster ions upon CI

particularly useful in locating double bonds. The EI and CI spectra of ammonia and isobutane reagent gas are compared in Fig. 7.6.

Isobutane is an especially versatile reagent gas, because (*i*) it provides low-fragmentation PICI spectra of all but the most nonpolar analytes, (*ii*) gives almost exclusively one well-defined adduct ($[M+C_4H_9]^+$, [M+57]) if any (Fig. 7.7), and (*iii*) can also be employed for electron capture negative ionization (Sect. 7.4).

Cluster ions

Cluster ions are formed by the agglomeration of polar species, mostly molecules, around an ion as a common center of charge, thereby essentially creating a solvent sphere around that ion. Cluster ions occur when a sufficiently large number of ion–neutral collisions provides the occasion. Cluster ions are therefore frequently formed in CI with polar reagent gases, from liquid matrices (Chap. 10), and generally when analytes at high concentration are subjected to soft ionization. Typical examples of cluster ions are $[(H_2O)_n+H]^+$, $[(NH_3)_n+H]^+$, $[nM+H]+$, etc. Cluster ions may also be generated by ionization of neutral clusters.

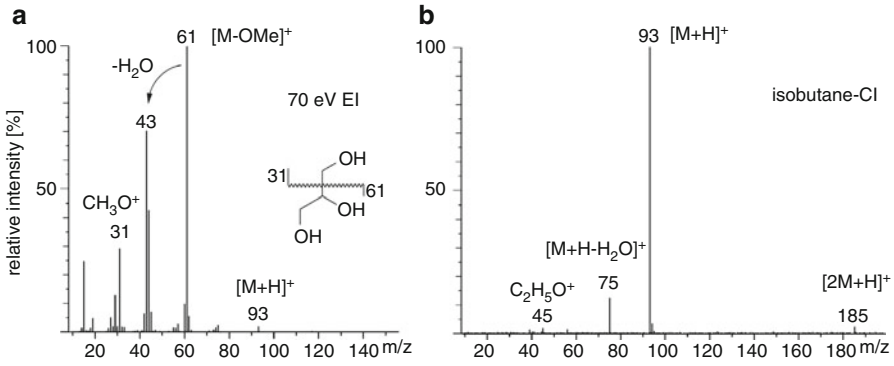

Fig. 7.7 70-eV EI (**a**) vs. isobutane-PICI spectrum of glycerol (**b**). Even in EI mode, an $[M+H]^+$ ion by autoprotonation is observed rather than $M^{+\bullet}$. Besides $[M+H]^+$, the PICI spectrum shows only few fragment ions and a weak $[2M+H]^+$ cluster ion signal

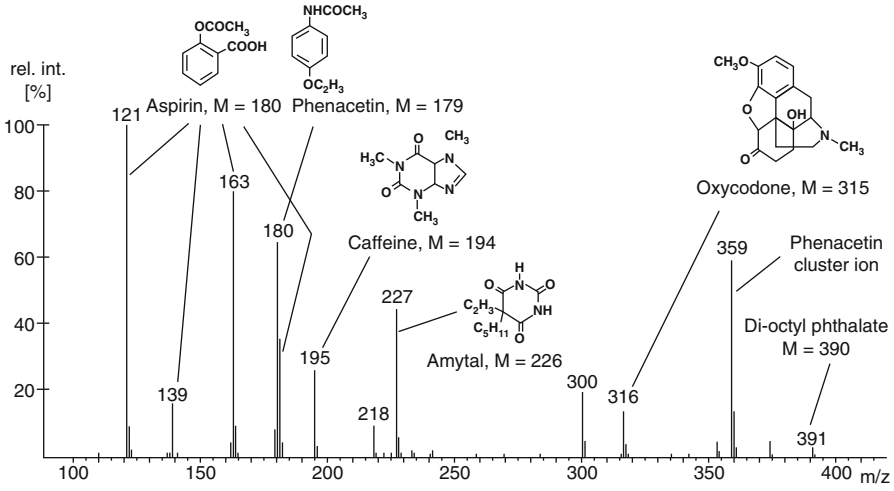

Fig. 7.8 Isobutane PICI mass spectrum of gastric contents in an overdose case (Reproduced from Ref. [33] by permission. © American Chemical Society, 1970)

Quick clinical diagnosis In a drug overdose case evidence was available of ingestion of Percodan (a mixture of several common drugs). The isobutane-PICI spectrum of the gastric extract was obtained (Fig. 7.8) [33]. All drugs formed an $[M+H]^+$ ion. Due to the low exothermicity of protonation by the *tert*-$C_4H_9^+$ ion, most $[M+H]^+$ ions did not fragment, solely that of aspirin showed intense fragment ion peaks that can be assigned as $[M+H–H_2O]^+$, *m/z* 163; $[M+H–H_2C{=}CO]^+$, *m/z* 139; and $[M+H–CH_3COOH]^+$, *m/z* 121. Phenacetine, in addition to the $[M+H]^+$ ion at *m/z* 180, formed a $[2M+H]^+$ cluster ion, *m/z* 359.

The spectra in both Figs. 7.7 and 7.8 tell us some important facts:

- Cluster ions like $[2M+H]^+$ are frequently formed in CI-MS and this needs to be considered when interpreting CI spectra of unknown samples.
- Today, in an overdose case one would perform the analysis by LC-MS in combination with other soft ionization techniques, but this example from 1970 demonstrates the softness of PICI.
- In addition, Fig. 7.8 may serve as an eye-opener for what can be achieved in mixture analysis when fragmentation is virtually absent and most or preferably all ions correspond to intact molecular species contained in a mixture (Sects. 14.7 and 14.8).

7.3 Proton Transfer Reaction-Mass Spectrometry

By combining the principles of PICI with an apparatus derived from *selected-ion flow tube* (SIFT) experiments, the technique of *proton transfer reaction-mass spectrometry* (PTR-MS) has been developed as a dedicated tool for the analysis of *volatile organic compounds* (VOCs) at parts-per-trillion by volume (pptv) level in air [53, 54]. PTR-MS is highly useful as a fast and quantitative method for the determination of VOCs as proven by numerous applications in food control, environmental and atmospheric research, as well as in medicine, e.g., to analyze the exhaled breath of patients [53–57]. Recent instrumental developments in PTR-MS result in even higher sensitivity for trace component analysis [58, 59].

7.3.1 Reagent ion Formation in PTR-MS

When water vapor is passed through the discharge of a hollow-cathode ion source it is ionized by primary electrons, basically by EI. Due to ion–molecule reaction sequences the product ion mixture forms H_3O^+ ions with high selectivity of up to 99.5% (Sect. 7.2.5) [53, 54]. Even $N_2^{+\bullet}$ or N^+ ions from nitrogen rapidly react with water molecules in the source region to result in more H_3O^+ ions. Thus, a high (typical count rates of $\approx 10^6$ counts s^{-1}) and almost pure flux of hydronium primary ions is provided that may then serve as reagent ions in a PICI process:

$$M + H_3O^+ \rightarrow [MH]^+ + H_2O \tag{7.15}$$

Fortunately this proton transfer reaction can generally occur for all VOCs as their *PA*s exceed that of water ($PA_{water} = 697$ kJ mol^{-1}) allowing for their exothermic protonation.

7.3.2 Analyte Ion Formation in PTR-MS

Different from classical CI sources, PTR-MS separates reagent ion generation from the stage of analyte ion formation. For the latter step, PTR-MS makes use of an ion flow tube

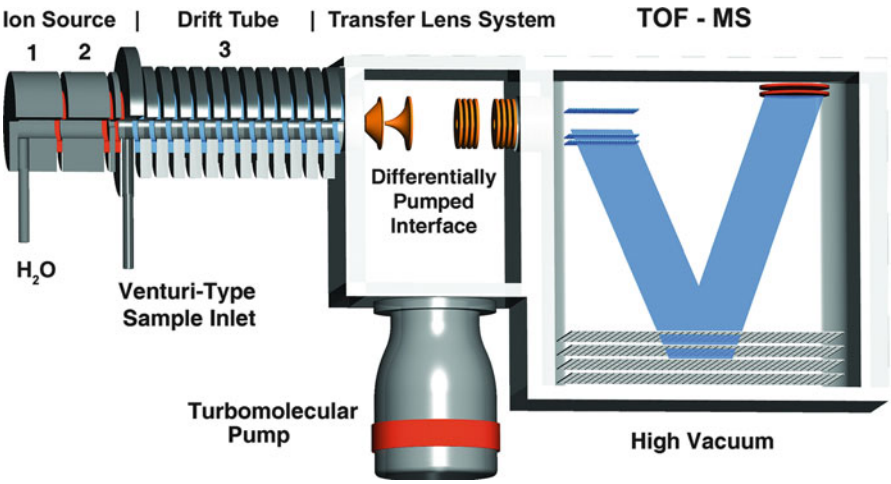

Fig. 7.9 PTR mass spectrometer. The ion source of the Ionicon PTR-TOF 2000™ is divided into a compartment for reagent ion generation from H_2O by (*1*) a hollow cathode and (*2*) a source drift region in front of the sample inlet, and (*3*) the drift tube for analyte ion formation. The TOF analyzer has its own turbomolecular pump to maintain high vacuum (*not shown*) (By courtesy of Ionicon Analytik GmbH, Innsbruck, Austria)

similar to a device used in IMS (Sect. 4.10), which provides sufficient time for effective reactions according to Eq. 7.14. Thus, ions are extracted from the hollow-cathode source, passed through a short drift region, and delivered to the extended reaction region, at the entrance of which the sample air containing the VOCs is continuously admitted (Fig. 7.9). Due to the purity of the H_3O^+ reagent ions delivered, there is no need for an ion flux-limiting quadrupole system to preselect reagent ions [53, 54].

On its way from the Venturi-type inlet to the downstream end of the drift section, H_3O^+ ions undergo nonreactive and reactive collisions with any one of the components of air [53, 54]. The water reagent gas PICI process causes the analyzed VOCs to be converted into $[M+H]^+$ ions.

The flow tube, which is about 20 cm long, acts as a reaction region that is maintained at about 1 mbar by action of a vacuum pump attached to its exit. These conditions afford thermalization and effective proton transfer as the hydronium ions drift along together with the VOC-loaded air. As PTR-MS does not necessitate an additional buffer gas, the analyte air is not diluted any further, a feature that contributes to the high sensitivity of the method. Furthermore, the original mole fraction of the analytes in the air is maintained.

VOCs in the Manaus area VOCs in air originate from natural (emission by plants and animals) and anthropogenic sources (usage of fossil fuels, evaporation of solvents, gases from landfill sites). Even without anthropogenic contributions, the Earth's atmosphere would consist of a complex mixture of VOCs [55]. Methane (2 pptv) is by far the most common organic compound in the Earth's atmosphere,

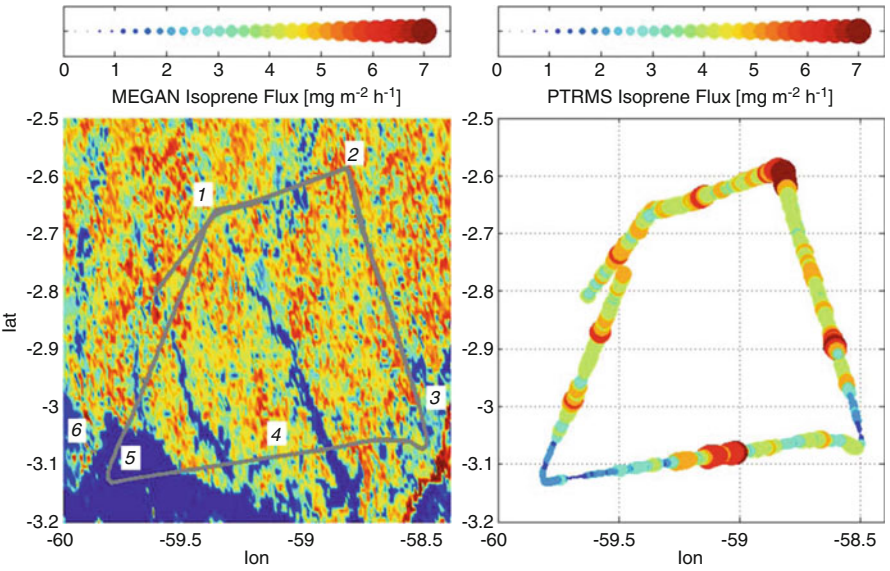

Fig. 7.10 Isoprene emission map generated for flight conditions from MEGAN (*left*) compared to airborne PTR-MS measurements (*right*). The *gray line* on the *left panel* depicts the flight track. Numbers *1–6* on the *left side* mark different land cover types: (*1*) mixed forest/plantation, (*2*) primary tropical forest, (*3*) soybean plantations, (*4*) mixed forest/plantation, (*5*) water, (*6*) Manaus urban region (Reproduced from Ref. [60] by permission. © The American Geophysical Union, 2007)

while other VOCs are in the ppbv range [55]. Isoprene, C_5H_8, and monoterpenes are important VOCs for modeling atmospheric chemistry in Amazonia [60]. The model of *emissions of gases and aerosols from nature* (MEGAN), estimates VOC fluxes and can describe the large observed variations associated with land-use change in the region of Manaus (Brasil). Airborne PTR-MS measurements of isoprene, detected as $[C_5H_9]^+$, m/z 69, were conducted by flying a racetrack pattern north-east of Manaus at constant altitude of 675 m above sea level. The racetrack of 320 km covered various landscapes such as primary forest, mixed water/forest, soybean plantations, and agricultural areas. In Fig. 7.9, the left panel depicts the isoprene emission map calculated from MEGAN, with the flight track plotted in gray. The right panel shows the surface flux calculated from airborne PRT-MS (Fig. 7.10) [60].

7.4 Charge Transfer Chemical Ionization

Charge transfer (CT) or *charge exchange* (CE) ionization occurs when an ion–neutral reaction takes place in which the ionic charge is transferred to the neutral [8]. In principle, any of the reagent systems discussed so far is capable of effecting

CT because the respective reagent molecular ions $X^{+\bullet}$ are also present in the plasma:

$$X^{+\bullet} + M \rightarrow M^{+\bullet} + X \tag{7.16}$$

With methane, isobutane, or ammonia, however, proton transfer is still prevailing. Therefore, reagent gases suitable for CT should exhibit abundant molecular ions even under the conditions of CI, whereas potentially protonating species have to be absent or at least of minor abundance.

CE or CE?
The acronym CE is also used for *capillary electrophoresis*, a separation method. CE may be coupled to a mass spectrometer via an electrospray interface (Chaps. 12 and 14), and thus CE-CI and CE-ESI-MS must not be confused. The term charge transfer (CT) avoids these ambiguities.

7.4.1 Energetics of CT

The energetics of CT is determined by the *ionization energy* of the neutral analyte, $IE_{(M)}$, and the *recombination energy* of the reagent ion, $RE_{(X+\bullet)}$. Recombination of an atomic or molecular ion with a free electron is the inverse of its ionization. $RE_{(X+\bullet)}$ is defined as the exothermicity of the gas phase reaction [7]:

$$X^{+\bullet} + e^{-} \rightarrow X \tag{7.17}$$

The recombination energy of the reagent ion $X^{+\bullet}$ is defined as the negative value of the corresponding heat of neutralization:

$$RE_{(X+\bullet)} = -\Delta H_r{}^0 \tag{7.18}$$

For monoatomic ions, the *RE* has the same numeric value as the *IE* of the neutral; for diatomic or polyatomic species differences may occur due to storage of energy in internal modes or electronic excitation. Ionization of the analyte via CT is effected if [61]:

$$RE_{(X+\bullet)} - IE_{(M)} > 0 \tag{7.19}$$

Now, the heat of reaction, and thus the minimum internal energy of the analyte molecular ion, is given by [62]:

$$E_{int(M+\bullet)} \geq RE_{(X+\bullet)} - IE_{(M)} \tag{7.20}$$

(The $\geq$ sign indicates the additional contribution of thermal energy.) In summary, no CT is expected if $RE_{(X+\bullet)}$ is less than $IE_{(M)}$; $M^{+\bullet}$ ions are predominantly expected if

$RE_{(X+\bullet)}$ is slightly above $IE_{(M)}$; extensive fragmentation occurs if $RE_{(X+\bullet)}$ is notably greater than $IE_{(M)}$ [62]. Accordingly, the "softness" of CTCI can be adjusted by choosing a reagent gas of suitable *RE*. Fortunately, the differences between *RE*s and *IE*s are small, and unless highest accuracy is required, *IE* data may be used to estimate the effect of a CT reagent gas (Table 2.1).

CTCI mass spectra closely resemble low-energy EI spectra (Sect. 5.6) because molecular ions are formed upon CT. As the sensitivity of CTCI is superior to low-energy EI [61], CTCI may be preferred over low-energy EI. The degree of fragmentation in CTCI is generally reduced as compared to EI because:

- The ion internal energy of the molecular ions is lower according to Eq. 7.20.
- The energy distribution is narrower, i.e., the high energy tail of the ion internal energy distribution as present in EI is cut off in CTCI.
- Some collisional cooling of the incipient molecular ions can occur that is not available in the strictly unimolecular regime of EI.

7.4.2 Reagent Gases for CTCI

Numerous gases are employed for CTCI. Reagent gases such as hydrogen [25] or methane can also affect CT. Typically, pure compounds are employed as CT reagent gases, but occasionally they are diluted with nitrogen to act as an inert or sometimes reactive buffer gas (Table 7.3). Compared to protonating CI conditions,

Table 7.3 CTCI reagent gases [7, 62, 65–68, 72]

Reagent gas	Reagent ion	*RE* or *RE* range [eV]
$C_6H_5NH_2$	$C_6H_5NH_2^{+\bullet}$	7.7
C_6H_5Cl	$C_6H_5Cl^{+\bullet}$	9.0
C_6H_6	$C_6H_6^{+\bullet}$	9.2
$NO^{\bullet} : N_2 = 1 : 9$	NO^+	9.3
$C_6F_6 : CO_2 = 1 : 9$	$C_6F_6^{+\bullet}$	10.0
$CS_2 : N_2 = 1 : 9$	$CS_2^{+\bullet}$	9.5–10.2
H_2S	$H_2S^{+\bullet}$	10.5
$COS : CO = 1 : 9$	$COS^{+\bullet}$	11.2
Xe	$Xe^{+\bullet}$	12.1, 13.4
N_2O (: $N_2 = 1 : 9$)	$N_2O^{+\bullet}$	12.9
CO_2	$CO_2^{+\bullet}$	13.8
CO	$CO^{+\bullet}$	14.0
Kr	$Kr^{+\bullet}$	14.0, 14.7
N_2	$N_2^{+\bullet}$	15.3
H_2	$H_2^{+\bullet}$	15.4
Ar	$Ar^{+\bullet}$	15.8, 15.9
Ne	$Ne^{+\bullet}$	21.6, 21.7
He	$He^{+\bullet}$	24.6

the reagent gas is typically admitted at somewhat lower pressure (15–80 Pa). Primary electron energies are reported in the 100–600 eV range.

The major reagent gases for CTCI are:

- benzene [47, 63, 64],
- chlorobenzene [65],
- carbon disulfide [66, 67],
- carbon oxysulfide [66–70],
- carbon monoxide [62, 66, 68],
- nitrogen [66],
- nitrogen oxide [62, 71],
- dinitrogen oxide [67, 71],
- argon [66], and
- xenon [66, 68].

CTCI of cyclohexene We want to compare the CTCI spectra of cyclohexene with the according 70-eV EI spectrum. Different CT reagent gases show different degrees of fragmentation (Fig. 7.11) [73]. The relative intensity of the molecular ion increases as the RE of the reagent gas decreases. As the sensitivity of CTCI is superior to low-energy EI [61], CTCI may be preferred over low-energy EI.

7.4.3 Compound Class-Selective CTCI

The energy distribution upon CT largely differs from that obtained upon EI in that the CT process delivers an energetically well-defined ionization of the neutral. Choosing the appropriate reagent gas allows for the selective ionization of a targeted compound class contained in a complex mixture [61, 64, 65, 74]. The differentiation is possible due to the characteristic range of *IE*s for each compound class. This property of CE-CI can also be applied to construct breakdown graphs (Sect. 2.11) from a set of CE-CI mass spectra by using reagent ions of stepwise increasing $RE_{(X+\bullet)}$, e.g., $C_6F_6^{+\bullet}$, $CS_2^{+\bullet}$, $COS^{+\bullet}$, $Xe^{+\bullet}$, $N_2O^{+\bullet}$, $CO^{+\bullet}$, $N_2^{+\bullet}$ [68, 72].

CTCI of fuels CTCI allows for the direct determination of the molecular weight distributions of the major aromatic components in liquid fuels and other petroleum products [61, 65, 74]. The approach involves selective CT between $C_6H_5Cl^{+\bullet}$ and the substituted benzenes and naphthalenes in the sample. In this application, chlorobenzene also serves as the solvent for the fuel to avoid interferences with residual solvent. Thus, the paraffinic components present in the fuel can be suppressed in the resulting CE-CI mass spectra (Fig. 7.12) [65].

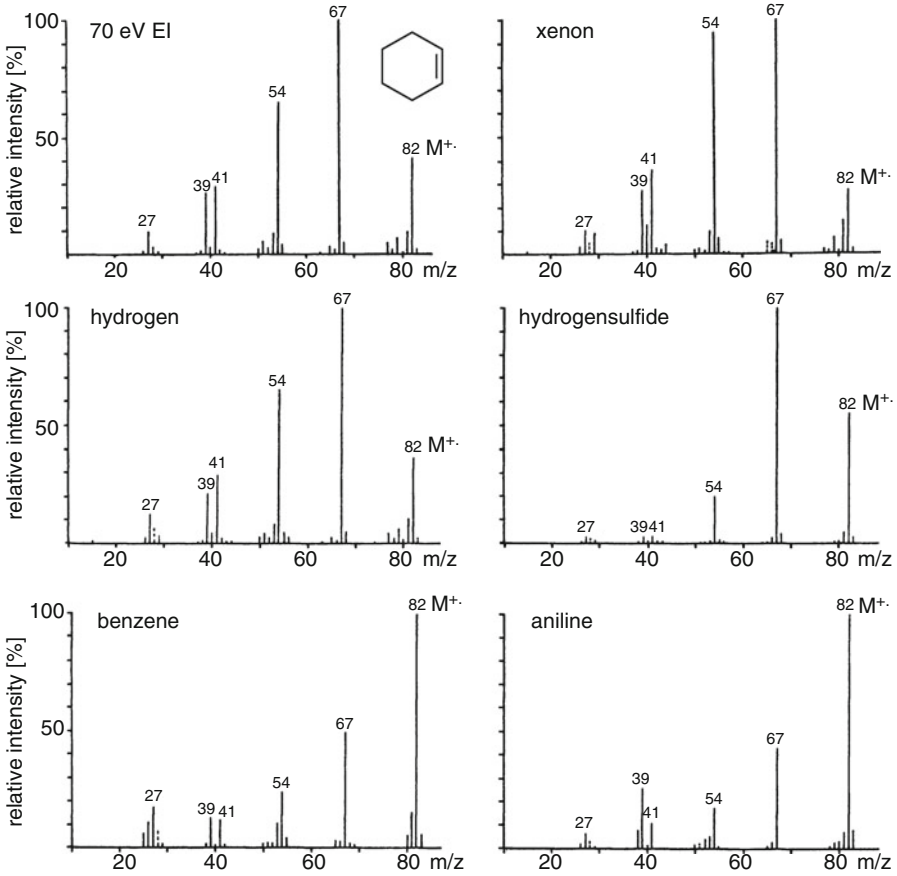

Fig. 7.11 Comparison of CTCI spectra of cyclohexene with that of the according 70-eV EI spectrum recorded with different reagent gases (Adapted from Ref. [73] by permission. © John Wiley & Sons, 1976)

7.4.4 Regio- and Stereoselectivity in CTCI

Small differences in activation energy, E_0, that exist between analogous fragmentations of regioisomers [66, 67, 69, 70] or stereoisomers do not cause significant differences in their 70-eV EI spectra. Pathways leading to a pair of different fragment ions cannot be distinguished, because minor differences in the respective *appearance energies* (*AE*s) are overridden by the excess energy of the fragmenting ions (Sect. 2.5). The situation changes if an energy-tunable ionization method is applied, which in addition offers a narrow internal energy distribution of the ions. Then, a significant alteration of relative intensities of a pair of fragments

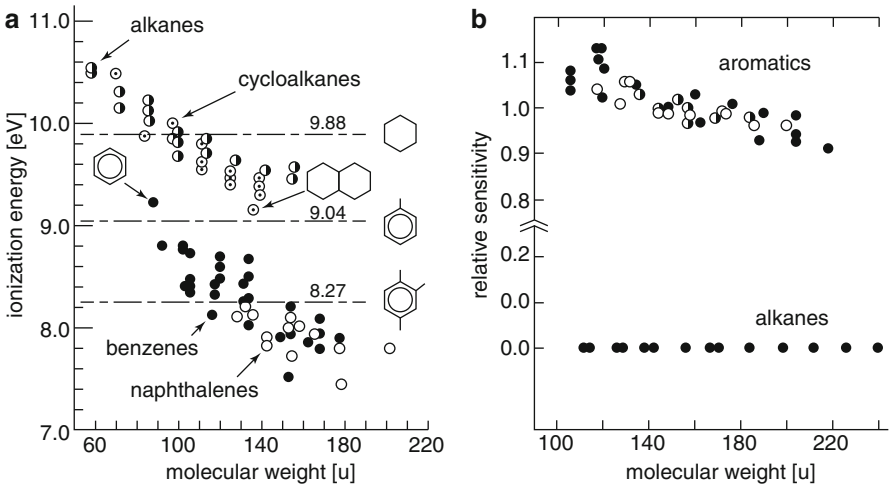

Fig. 7.12 (**a**) Ionization energies of certain classes of organic molecules as a function of their molecular weight, and (**b**) relative sensitivities for (○) alkylbenzenes, (●) polyolefines, and (◑) substituted naphthalenes in chlorobenzene CTCI (Adapted from Ref. [65] by permission. © American Chemical Society, 1983)

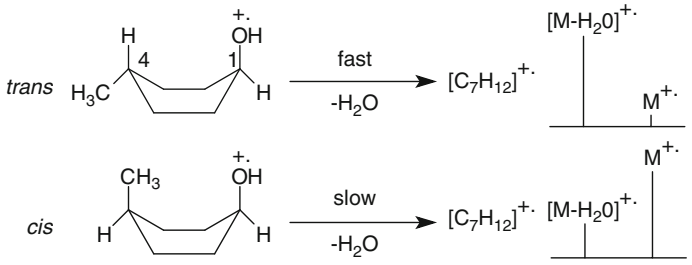

Scheme 7.2

could be effected if the appearance energies $AE_{(F1)}$ and $AE_{(F1')}$ of these fragments from isomeric precursors were just below $RE_{(x+\bullet)}$.

Distinguishing epimers In epimeric 4-methylcyclohexanols the methyl and the hydroxyl group can either both reside in axial position (*cis*) or one is equatorial and the other axial (*trans*). In the *trans* isomer, stereospecific 1,4–H_2O elimination should proceed easily (Sect. 6.11), while H_2O loss from the *cis* isomer is more demanding. CE-CI using $C_6F_6^{+\bullet}$ reagent ions clearly reveals the difference between these stereoisomers from the according $M^{+\bullet}/[M–H_2O]^{+\bullet}$ ratio determined as *trans* : *cis* = 0.09: 2.0 = 23) [72] (Scheme 7.2).

7.5 Negative-Ion Chemical Ionization

In any CI plasma, ions of both polarities, positive *and* negative, are formed simultaneously, e.g., $[M+H]^+$ and $[M–H]^-$ ions, and it is just a matter of the polarity of the acceleration voltage which ions are going to be extracted from the ion source [75]. Thus, from a technical point of view, *negative-ion chemical ionization* (NICI) [76] mass spectra can readily be obtained.

As in PICI, there are also several pathways in NICI leading to the formation of negative ions [77–80]. First, in case of acidic molecules, such as carboxylic acids [81], diimides, or phenols, there is dissociation leading to *deprotonation*:

$$M \rightarrow [M - H]^- + H^+ \tag{7.21}$$

While deprotonation can occur spontaneously, the presence of a proton-accepting base, B, either delivered by some species of the reagent gas or by the excess of other analyte neutrals (cf. autoprotonation, Sect. 7.2.1) accelerates the process:

$$M + B \rightarrow [M - H]^- + [BH]^+ \tag{7.21a}$$

Second, *nucleophilic addition*, i.e., anion attachment, can occur:

$$M + A^- \rightarrow [M + A]^- \tag{7.22}$$

Third, *ion-pair formation*, induced by direct interaction with an energetic electron (Sect. 2.1), can also play a role:

$$M + e^- \rightarrow [M - B]^- + B^+ + e^- \tag{7.23}$$

Nonetheless, ion-pair formation is generally the energetically least favorable process. Each of these processes delivers even-electron analyte anions.

Nucleophilic addition The NICI mass spectrum of tetraiodoethene, $I_2C = CI_2$, has been obtained using isobutane reagent gas (Fig. 7.13). The negative molecular ion, $M^{-\bullet}$, at *m*/*z* 531.6 has a relative intensity of just 0.15%, while the product of nucleophilic addition, $[M+I]^-$, *m*/*z* 658.5, yields the base peak [82]. Losses of $I^\bullet$ and I_2 from $M^{-\bullet}$ are also observed. The series of peaks at *m*/*z* 126.9, 253.8, and 380.7 corresponds to traces of iodine present as impurity of tetraiodoethene. The iodine is also ionized by both electron capture (EC, next paragraph) and iodide addition. The spectrum nicely exemplifies the superimposition of mass spectra of two components of a mixture. It is not always simple to tell the corresponding peaks apart; accurate mass measurements or tandem mass spectrometry may be required. It is worth noting the mass defect introduced by the iodine and the ^{13}C isotopic peak of merely 2% due to only two carbon atoms present.

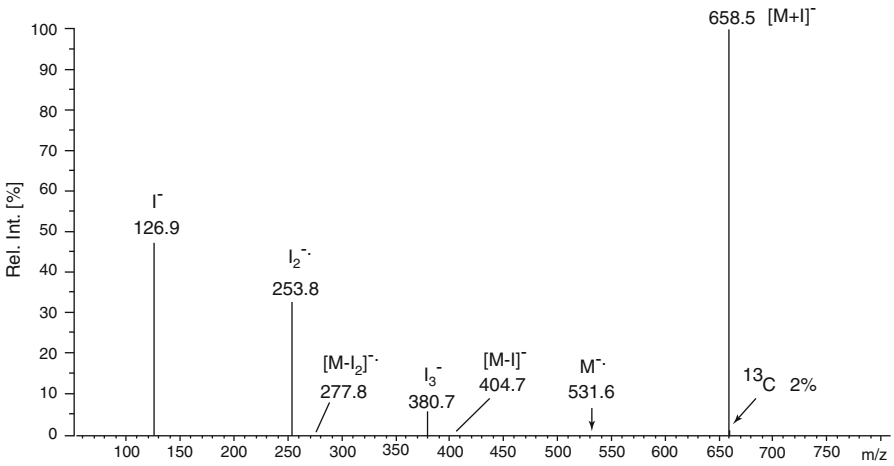

Fig. 7.13 NICI mass spectrum of tetraiodoethene (isobutane reagent gas, electron emission 300 µA at 200 eV, and ion source temperature of 200 °C) (Adapted from Ref. [82] with permission. © Wiley-VCH, Weinheim, 2007)

Competitors to classical NICI

Over the last decade, NICI applications have diminished because these analyses have mostly been carried out by negative-ion *atmospheric pressure chemical ionization* (APCI, Sect. 7.8). APCI is compatible with liquid chromatography (Chap. 14) and can readily be implemented on instruments with electrospray ionization interface (ESI, Chap. 12). Such instruments have an enormous market share, and thus, it is often more convenient and economic to switch between ESI and APCI as required. APCI will be dealt with a the end of this chapter.

7.6 Electron Capture Negative Ionization

There is one further process of negative-ion formation: *electron capture* (EC) or *electron attachment* [76]. EC is a resonance process whereby an electron of low kinetic energy is incorporated into an orbital of an atom or molecule [8]. The method employing this process is termed *electron capture negative ionization* (ECNI). Electron capture negative ionization is of special interest, because it provides superior sensitivity towards many toxic and/or environmentally relevant substances [83–87].

Strictly speaking, ECNI is not a subtype of NICI because the electrons are not provided by a reagent ion. In ECNI, the reagent gas solely serves as a moderator to

decelerate the energetic electrons injected from the filament to close to thermal energy. Nonetheless, the ion source conditions to achieve ECNI are the same as for NICI. In fact, the processes discussed in Eqs. 7.21, 7.22, and 7.23 often compete with EC, and thus, characteristics of NICI and ECNI can simultaneously appear in mass spectra [88].

7.6.1 Ion Formation by Electron Capture

When a neutral molecule interacts with an electron of high kinetic energy, the positive radical ion is generated by EI. If the electrons have less energy than the *IE* of the respective neutral, EI is prohibited. As the electrons approach thermal energy, EC can occur instead. Under EC conditions, there are three different processes of ion formation [78, 89–92].

First, *resonance electron capture* yields the negative molecular ion, $M^{-\bullet}$:

$$M + e^- \rightarrow M^{-\bullet} \tag{7.24}$$

Second, *dissociative electron capture* can result in fragment ion formation by immediate loss of a radical from the incipient molecular radical anion:

$$M + e^- \rightarrow [M - A]^- + A^\bullet \tag{7.25}$$

Third, *ion-pair formation* can also occur:

$$M + e^- \rightarrow [M - B]^- + B^+ + e^- \tag{7.26}$$

Molecular radical anions, $M^{-\bullet}$, are generated by capture of electrons with 0–2 eV kinetic energy, whereas fragment ions are generated by capture of electrons from 0 to 15 eV. Ion-pair formation tends to occur when electron energies exceed 10 eV [91]. Odd-electron molecular anions are exclusively formed by resonance electron capture, whereas even-electron fragment ions are formed by dissociative electron capture and ion-pair formation.

7.6.2 Energetics of Electron Capture

The potential energy curves of a neutral molecule AB and the potential ionic products from Eqs. 7.24, 7.25, and 7.26 are compared below (Fig. 7.14). These graphs reveal that the formation of negative molecular ions, $AB^{-\bullet}$, is energetically more favorable than homolytic bond dissociation of AB and that the $AB^{-\bullet}$ ions have internal energies close to the activation energy for dissociation [76, 78, 89]. The negative molecular ions from EC are therefore definitely less excited than their positive counterparts from 70-eV EI.

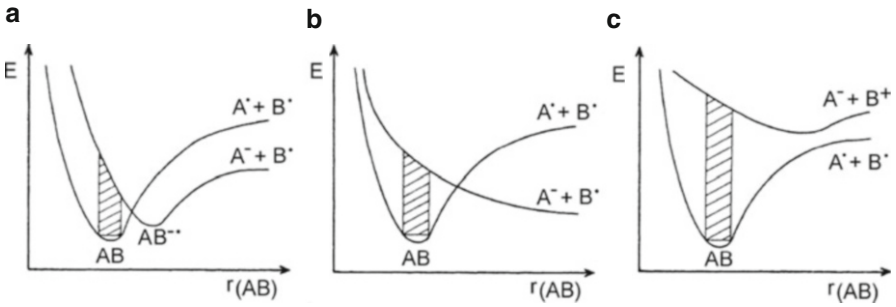

Fig. 7.14 Energetics of (**a**) resonance electron capture, (**b**) dissociative electron capture, and (**c**) ion-pair formation (Adapted from Ref. [89] by permission. © John Wiley & Sons, 1981)

Fig. 7.15 EC spectrum of benzo[a]pyrene (isobutane buffer gas, ion source 200 °C). The two additional minor signals correspond to impurities of the sample

EC of benzo[a]pyrene The EC mass spectrum of benzo[a]pyrene, $C_{20}H_{12}$, shows the negative molecular ion exclusively at *m/z* 252 (Fig. 7.15). This spectrum is representative for EC spectra of *polycyclic aromatic hydrocarbons* (PAHs) [93, 94]. One particular PAH, fluoranthene, has recently received much attention as its $M^{-\bullet}$ ion serves as electron donating reagent ion in *electron transfer dissociation* (ETD, Sect. 9.15).

The energetics of the EC process $M + e^- \rightarrow M^{-\bullet}$ (Eq. 7.24) are determined by the *electron affinity* (*EA*) of the neutral. The electron affinity is the negative of the enthalpy of the attachment of a zero kinetic energy electron to a neutral molecule or atom:

$$-\Delta H_r = EA_{(M)} \tag{7.27}$$

Just like the *IE* of a molecule is governed by the atom of lowest *IE* within that neutral (Sect. 2.1), the *EA* of a molecule is basically determined by the atom of

Table 7.4 Selected electron affinities [97]

Compound	*EA* [eV]	Compound	*EA* [eV]
Carbon dioxide	–0.600	Pentachlorobenzene	0.729
Naphthalene	–0.200	Tetrachloromethane	0.805
Acetone	0.002	Biphenylene	0.890
1,2-Dichlorobenzene	0.094	Nitrobenzene	1.006
Benzonitrile	0.256	Octafluorocyclobutane	1.049
Molecular oxygen	0.451	Pentafluorobenzonitrile	1.084
Carbon disulfide	0.512	2-Nitronaphthalene	1.184
Benzo[e]pyrene	0.534	1-Bromo-4-nitrobenzene	1.292
Tetrachloroethylene	0.640	Antimony pentafluoride	1.300

highest electronegativity. This is why analytes with halogens, in particular fluorine and chlorine, as well as with nitro groups make attractive candidates for EC (Table 7.4) [95]. If EC occurs with a neutral of negative *EA*, the electron–molecule complex will have a short lifetime (*autodetachment*), but in case of positive *EA* a negative molecular ion can persist.

Dissociative EC Consider the dissociative EC process $CF_2Cl_2 + e^- \rightarrow F^- + CFCl_2^{\bullet}$ and let the potential energy of CF_2Cl_2 be zero. The homolytic bond dissociation energy $D_{(F–CFCl2)}$ has been calculated as 4.93 eV. Now, the potential energy of the products is 4.93 eV less the electron affinity of a fluorine atom ($EA_{(F^{\bullet})} = 3.45$ eV), i.e., the process is endothermic by 1.48 eV. The experimental *AE* of the fragments is 1.80 eV. This yields a minimum excess energy of 0.32 eV (Fig. 7.16) [96].

7.6.3 Creating Thermal Electrons

Thermionic emission from a heated metal filament is the standard source of free electrons. However, after acceleration into the ion source, those electrons usually carry 10–200 eV rather than thermal energy (0.1–1 eV) and need to be decelerated for EC. Buffer gases such as methane, isobutane, or carbon dioxide serve well for that purpose, but others have also been used [77, 88, 98]. These gases do not form negative ions themselves while effectively moderating the energetic electrons to thermal energy [84]. Despite inverse polarity of the extraction voltage, the same conditions as for PICI in terms of buffer gas pressure, ion source temperature, and energy of primary electrons can usually be applied. Lowering the ion source temperature provides lower-energy electrons, e.g., assuming a Maxwell-Boltzmann energy distribution the mean electron energy is 0.068 eV at 250 °C and 0.048 eV at 100 °C [84].

Alternatively to direct supply from a heated filament, electrons of well-defined low energy can be delivered into the ion volume by an electron monochromator [92, 96, 99–101].

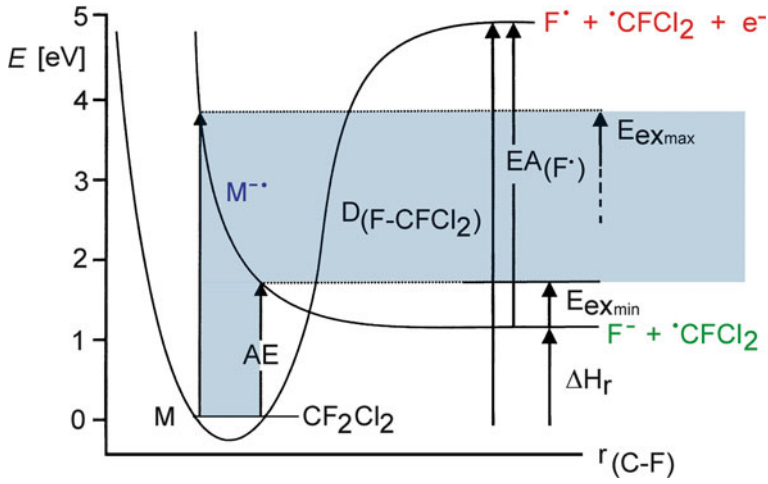

Fig. 7.16 Potential energy diagram of the dissociative EC process of dichloro-difluoromethane. The molecular radical anion (*blue*) does not possess a minimum on the energy surface but immediately dissociates via $CF_2Cl_2 + e^- \rightarrow F^- + CFCl_2^\bullet$ (*green products*), whereas the competing formation of two radicals is outside the energy window (*red products*)

NICI and ECNI in practice

Both NICI and ECNI are comparatively sensitive to ion source conditions [80, 100]. The actual ion source temperature, the buffer gas, the amount of sample introduced, and ion source contaminations each play important roles. Regular cleaning of the ion source is important [85]. It much depends on the actual analyte and instrument setting which of the competing processes outlined in Eqs. 7.21, 7.22, 7.23, 7.24, 7.25, and 7.26 finally prevails. Interlaboratory comparisons of NICI and ECNI spectra are therefore not as reliable as in case of 70-eV EI spectra.

7.6.4 Appearance of ECNI Spectra

ECNI spectra generally exhibit strong molecular ions and no primary fragment ions (Fig. 7.15) or in some cases just a few (Fig. 7.17). As $M^{-\bullet}$ is an odd-electron species, homolytic bond cleavages as well as rearrangement fragmentations may occur. Apart from the opposite charge, there are close similarities to the fragmentation pathways of positive molecular ions (Chap. 6) [80, 90, 91].

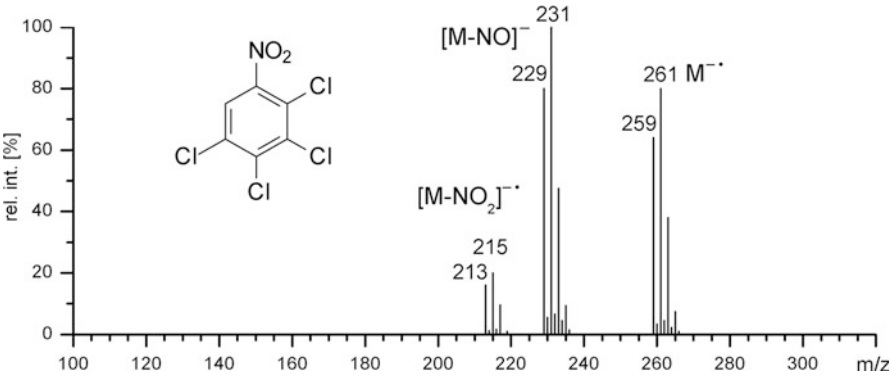

Fig. 7.17 Methane EC spectrum of 2,3,4,5-tetrachloronitrobenzene (Redrawn from Ref. [91] by permission. © John Wiley & Sons, 1988)

ECNI spectrum of PFK Perfluorokerosine (PFK), a mixture of numerous perfluorinated compounds, is frequently employed as mass calibrant in EI where it delivers spectra that almost exclusively represent $[C_nF_{2n-1}]^+$ fragment ions like $[C_5F_9]^+$, *m/z* 231 (Sect. 3.6.2). In ECNI, the situation changes because low-energy molecular anions are formed, a large fraction of which does not undergo fragmentation (Fig. 7.18). Roughly the upper half of the ECNI spectrum of PFK is thus made up by peaks at even *m/z* values while the lower half shows $[C_nF_{2n-1}]^-$ fragment ions fragment ion peaks of similar intensity at odd *m/z* values, e.g., $[C_5F_9]^-$, *m/z* 231, or $[C_6F_{11}]^-$, *m/z* 281 (cf. nitrogen rule, Sect. 6.2.7). The peak at *m/z* 153.1 is caused by residual nitrobenzyl alcohol that had been used the previous day as a matrix in fast atom bombardment (Chap. 10) on this instrument.

7.6.5 Applications of ECNI

ECNI, especially when combined with GC-MS (Sects. 14.2, 14.3, and 14.4), is commonly used in the monitoring of halogenated compounds and nitrocompounds as often represented in environmental pollutants such as dioxins [96, 100, 101], pesticides [96], halogenated metabolites [86], food contaminants [102, 103], DNA adducts [95], explosives [79, 104, 105], and others [83, 84, 106–108].

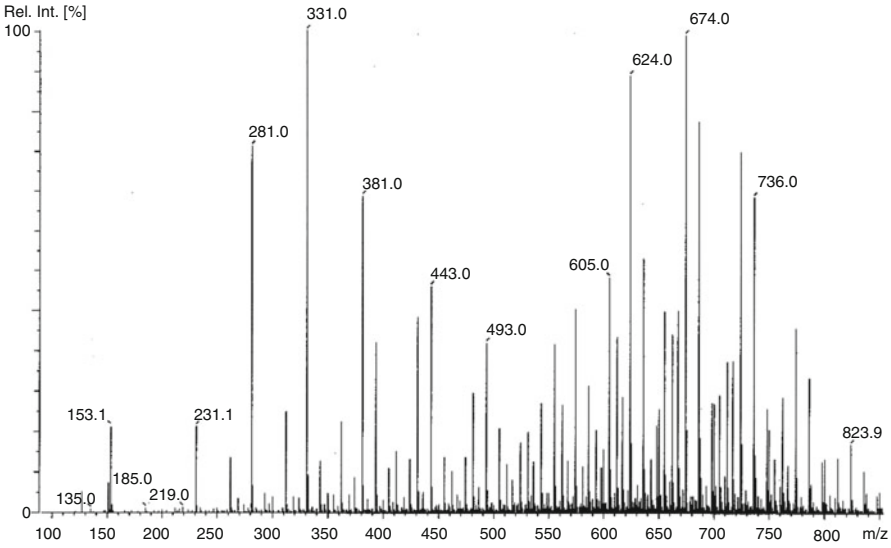

Fig. 7.18 ECNI spectrum of perfluorokerosene (PFK) as obtained with isobutane buffer gas. While fragment ions prevail in the lower half of the *m*/*z* range, molecular ions of the numerous constituents are characteristic of the upper half

7.7 Desorption Chemical Ionization

In CI, the analyte is generally introduced into the ion source via *direct insertion probe* (DIP), *gas chromatograph* (GC), or *reservoir inlet* (Sect. 5.2). However, CI can also be used in conjunction with sample introduction by a *direct exposure probe* (DEP). This is known as *desorption chemical ionization* (DCI) [34, 109, 110]. In DCI, the analyte is applied from solution or suspension to the outside of a thin resistively heated wire loop or coil. Then, the analyte is directly exposed to the reagent gas plasma while being rapidly heated at rates of several hundred °C s^{-1} and to temperatures up to about 1500 °C (Sect. 5.2). The analytical result depends on the actual shape of the wire, the sample application method, and the heating rate [111, 112]. The rapid heating of the sample plays an important role in promoting molecular species rather than pyrolysis products [113]. In contrast to *desorption electron ionization* (DEI), DCI is more frequently applied [112, 114–116]. An appropriate experimental setup provided, accurate mass measurements can be achieved in DCI mode [117].

Pyrolysis DCI of cellulose The pyrolysis (Py) DCI mass spectrum of cellulose, H$(C_6H_{10}O_5)_nOH$, as acquired using NH_3 reagent gas, 100 eV of electron energy, and scanning *m*/*z* 140–700 at 2 s per cycle shows a series of distinct signals. The peaks are separated by 162 u, i.e., by $C_6H_{10}O_5$ saccharide units. The main signals are due

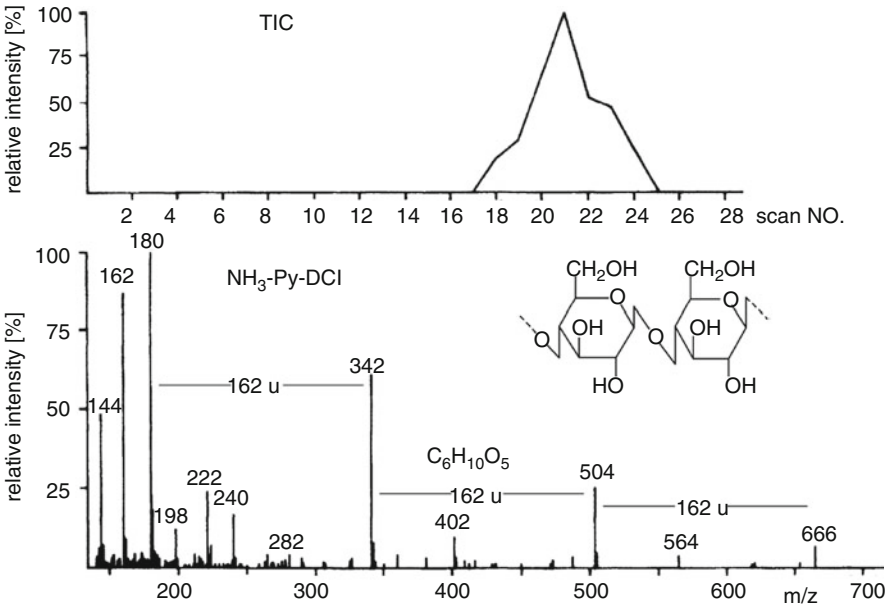

Fig. 7.19 Ammonia-Py-DCI mass spectrum of cellulose and total ion current (Adapted from Ref. [111] by permission. © Research Council of Canada, 1994)

to ions from anhydro-oligosaccharides, $[(C_6H_{10}O_5)_n+NH_4]^+$, formed upon heating of the cellulose in the ammonia CI plasma (Fig. 7.19) [111].

Other terms

Although *desorption chemical ionization* being the correct term [112], DCI is sometimes referred to as *direct CI*, *direct exposure CI*, *in-beam CI*, or even *surface ionization*. Nowadays, DCI is rarely used, because in most instances one of the various desorption/ionization methods serves the purpose much better (Chaps. 8, 10, 11, 12 and 13).

7.8 Atmospheric Pressure Chemical Ionization

Up to this point, we have exclusively dealt with ionization in (high) vacuum. The attempt for online mass spectrometric detection for liquid chromatographic separations (Sects. 14.1 and 14.5) initiated the development of a wealth of ionization methods and interfaces permitting ionization at atmospheric pressure to be directly and continuously attached to high vacuum mass analyzers.

7.8.1 Atmospheric Pressure Ionization

Atmospheric pressure ionization (API) was the first technique to directly connect solution phase analyte supply with a mass analyzer [118]. In API, a dilute solution of the analyte is injected at atmospheric pressure into a stream of hot nitrogen (≈200 °C) to rapidly evaporate the solvent. The vapor passes through a tube bearing radioactive ^{63}Ni, a β emitter (Fig. 7.20). The electrons emitted by ^{63}Ni induce a complex sequence of reactions finally delivering reagent ions for chemical ionization. Thus, starting with the ionization of N_2, consecutive ion–molecule reactions eventually lead to the formation of $[(H_2O)_n+H]^+$ cluster ions:

$$N_2 + e^- \rightarrow {N_2}^{+\bullet} + 2e^- \tag{7.28}$$

$${N_2}^{+\bullet} + N_2 + N_{2(\text{3rd body})} \rightarrow {N_4}^{+\bullet} + N_{2(\text{3rd body})} \tag{7.29}$$

$${N_4}^{+\bullet} + H_2O \rightarrow {H_2O}^{+\bullet} + 2N_2 \tag{7.30}$$

$${H_2O}^{+\bullet} + H_2O \rightarrow H_3O^+ + OH^\bullet \tag{7.31}$$

$$H_3O^+ + H_2O \rightarrow \left[(H_2O)_2 + H\right]^+ \tag{7.32}$$

Here, only the first step of $[(H_2O)_n+H]^+$ cluster ion formation is explicitly formulated. As the *PA* of H_2O (697 kJ mol^{-1}) is essentially below that of any

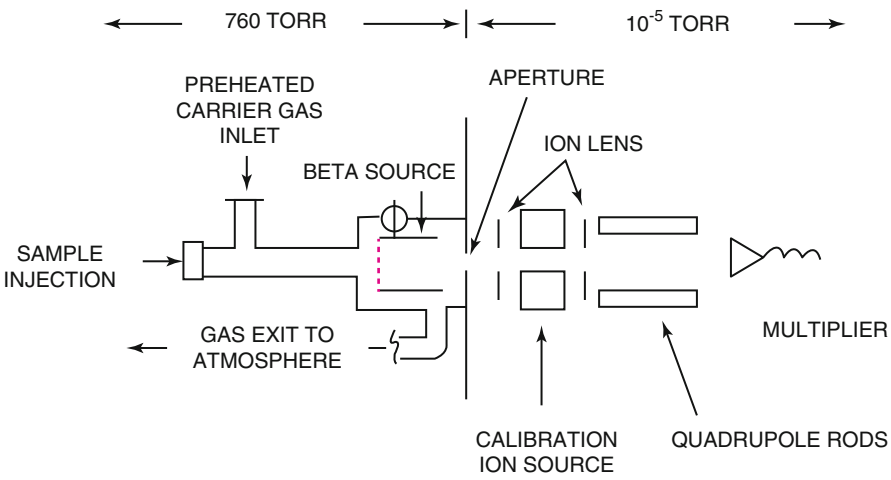

Fig. 7.20 The original implementation of API. Here, primary electrons are delivered by a ^{63}Ni foil. For API, the filament of the EI calibration source was switched off and only the electrostatic lenses where used to pass the ions into the quadrupole mass analyzer chosen for its tolerance to moderate vacuum conditions (Reproduced from Ref. [118] with permission. © The American Chemical Society, 1973)

organic molecule that could be of interest as potential analyte (Table 2.6), water cluster ions protonate the analyte molecules by a chemical ionization process at atmospheric pressure [118–120]:

$$[H_2O)_n + H]^+ + M \rightarrow [M + H]^+ + nH_2O \tag{7.33}$$

Always the same reaction
Did you notice that the reaction $H_2O^{+\bullet} + H_2O \rightarrow H_3O^+ + OH^\bullet$ (Eq. 7.31) follows the same pattern as does the reaction $CH_4^{+\bullet} + CH_4 \rightarrow CH_5^+ + CH_3^\bullet$ (Eq. 7.6) that is relevant for PICI using methane reagent gas? In fact, this general reaction, $M^{+\bullet} + M \rightarrow [M+H]^+ + [M–H]^\bullet$, is observed whenever a molecular ion is formed in an excess of neutral molecules of the same species, provided the number of collisions during its lifetime permits ion–molecule reactions to occur.

7.8.2 Atmospheric Pressure Chemical Ionization

Ion sources using a radioactive ^{63}Ni foil are not ideally suitable for the common laboratory as the occasional need for abrasive cleaning of the source inevitably leads to radioactive contamination. The Horning group thus refined API by replacing ^{63}Ni, the primary source of ionization, with a corona discharge [121, 122]. The reagent ion plasma is now maintained by a corona discharge between the sharp tip of a needle and the spray chamber walls serving as the counter electrode. The improved technique providing enhanced primary ion formation was termed *atmospheric pressure chemical ionization* (APCI). Basically, APCI represents an atmospheric-pressure variant of "classical" vacuum chemical ionization. In contrast to CI, ion–molecule reactions occurring at atmospheric pressure are employed for analyte ion production.

Nebulization of the analyte solution is effected by action of the pneumatic nebulizer. The transformation of the aerosol into a vapor composed of solvent and highly diluted sample is then performed in a heater cartridge set to about 500 °C (Fig. 7.21).

In APCI, the ions are transferred into the mass analyzer by use of the same atmosphere-to-vacuum interface as employed in electrospray ionization (ESI), the design of which will be pointed out along with the development of ESI (Sect. 12.2). As a benefit, ESI sources can easily be switched to APCI operation. To do so, the ESI spray head is exchanged for a unit comprising a pneumatic nebulizer and a heated spray chamber with a needle electrode mounted in front of the sampling orifice, while the atmosphere-to-vacuum interface stays in place [123–125].

Older APCI sources require a liquid flow of 200–1000 µl min^{-1} for effective vaporization and ionization. While this is fine for liquid chromatography coupling,

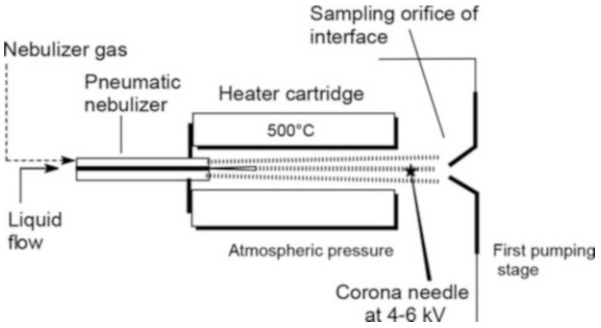

Fig. 7.21 APCI source. The liquid flow is pneumatically sprayed into a heated vaporizer where ionization is initiated by a corona discharge at atmospheric pressure. The atmospheric pressure-to-vacuum interface serves appropriately for all types of API techniques without any alterations

direct injection using a syringe pump is hampered by such a high flow. More recent APCI source designs also permit stable operation using a liquid flow of just 5–20 µl min^{-1}. Typical corona discharge currents are in the order of 10 µA, and thus, the blueish discharge is only visible in virtual darkness (Fig. 7.22).

API techniques
Atmospheric pressure ionization as originally devised in 1973 has never been widely applied as it was almost immediately replaced by atmospheric pressure chemical ionization. Nonetheless, *atmospheric pressure ionization* has survived as a collective term to encompass the manifold ionization methods employing analyte ion formation at atmospheric pressure.

7.8.3 Positive Ion Formation in APCI

Apart from initiation by a corona discharge, the pathway of reagent ion formation in APCI follows the route just discussed in API:

$$\text{corona discharge} + N_2 \rightarrow {N_2}^{+\bullet} + e^- \tag{7.34}$$

$${N_2}^{+\bullet} + N_2 + N_{2(\text{3rd body})} \rightarrow {N_4}^{+\bullet} + N_{2(\text{3rd body})} \tag{7.35}$$

$${N_4}^{+\bullet} + H_2O \rightarrow 2N_2 + {H_2O}^{+\bullet} \tag{7.36}$$

Ion–molecule reactions are fast at atmospheric pressure because collision rates are in the order of 10^9 s^{-1}. Seemingly bimolecular reactions can in fact be termolecular, because a neutral collision partner like N_2 in Eq. 7.35 is required for immediate removal of excess energy (Table 7.5) [126–128].

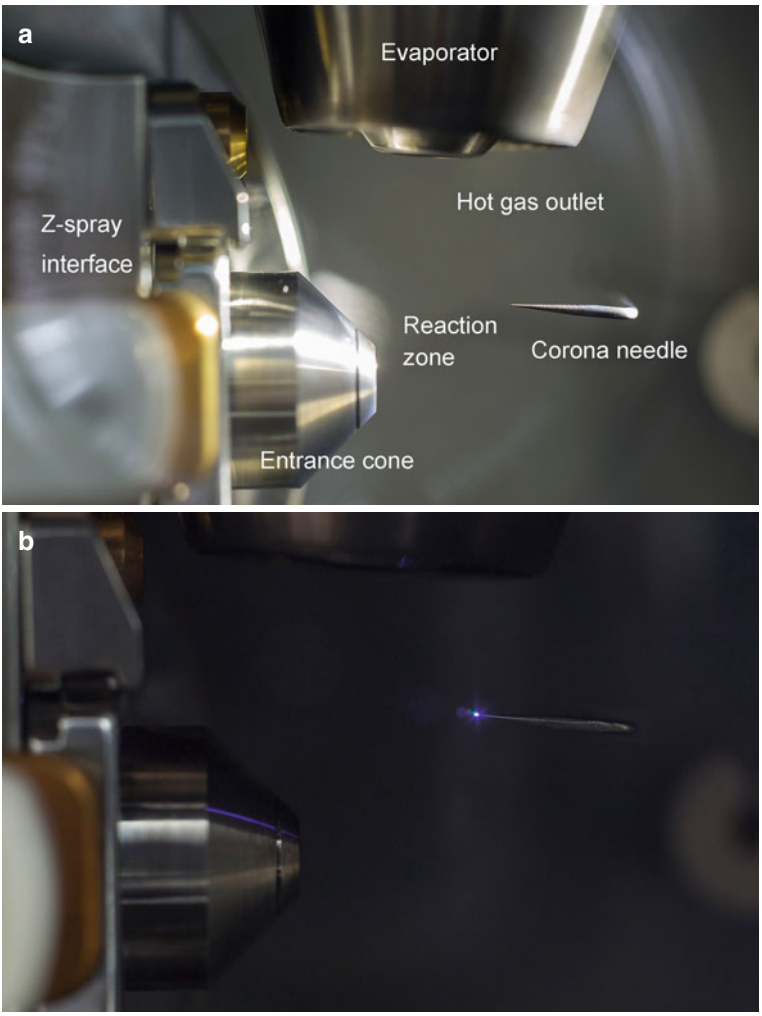

Fig. 7.22 APCI source of a Waters SQD2 instrument attached to a Z-spray interface. (**a**) APCI source as seen in daylight, (**b**) shaded source in operation. The blueish corona discharge corresponding to about 10 μA discharge current at the tip of the needle is only visible in virtual darkness

Table 7.5 Comparison of typical conditions and occurrence of elementary processes in atmospheric pressure ionization and vacuum ionization techniques

Parameter or reaction	API methods	Vacuum ionization
Pressure	1000 mbar	10^{-6} mbar
Mean free molecular path	100 nm	100 m
Hard sphere collision number	10^{9} s^{-1}	1 s^{-1}
Number density of O_2	10^{14}–10^{18} molecules cm^{-3}	10^{4}–10^{7} molecules cm^{-3}
Number density of H_2O	10^{13}–10^{16} molecules cm^{-3}	10^{3}–10^{6} molecules cm^{-3}
Source residence time of ions	10 ms to 1 s	1 µs
Unimolecular decay of ions	None to rarely	Yes
Bimolecular reactions	Yes	No
Termolecular reactions	Yes	No

Reprinted from Ref. [128] with permission. © Springer, 2014

Next, the $H_2O^{+\bullet}$ ions rapidly form cluster ions:

$$H_2O^{+\bullet} + H_2O \rightarrow H_3O^{+} + OH^{\bullet} \tag{7.37}$$

$$H_3O^{+} + nH_2O \rightarrow \left[(H_2O)_n + H\right]^{+} \tag{7.38}$$

The $[(H_2O)_n + H]^+$ ions then act as reagent ions [127]:

$$M + \left[(H_2O)_n + H\right]^{+} \rightarrow [M + H]^{+} + nH_2O \tag{7.39}$$

The concentration of water in the actual atmosphere of the reaction zone as well as the dwell time exert a strong influence on the $[(H_2O)_n + H]^+$ cluster ion distribution (Fig. 7.23) [128]. The relative contribution of the individual $[(H_2O)_n + H]^+$ cluster ions on the process of analyte ion formation may thus be subject to wide variation.

Ammonium adducts are frequent in APCI of medium polar compounds. $[M+NH_4]^+$ ions are observed, for example, with oxygen-rich molecules, in particular in absence of basic functional groups, e.g., polyethylene glycols, ketones, di-or triacylglycerols, and polysiloxanes:

$$M + [NH_4]^{+} \rightarrow [M + NH_4]^{+} \tag{7.40}$$

Ammonium ions may be delivered along with the sample or can be formed from trace amounts of ammonia in the atmosphere.

Common reaction scheme

The same sequence of reactions, although initiated by different sources of primary ionization, is observed not only in APCI but also in *atmospheric pressure photoionization* (APPI, Sect. 7.9) and *direct analysis in real time* (Sect. 13.8) [127, 129].

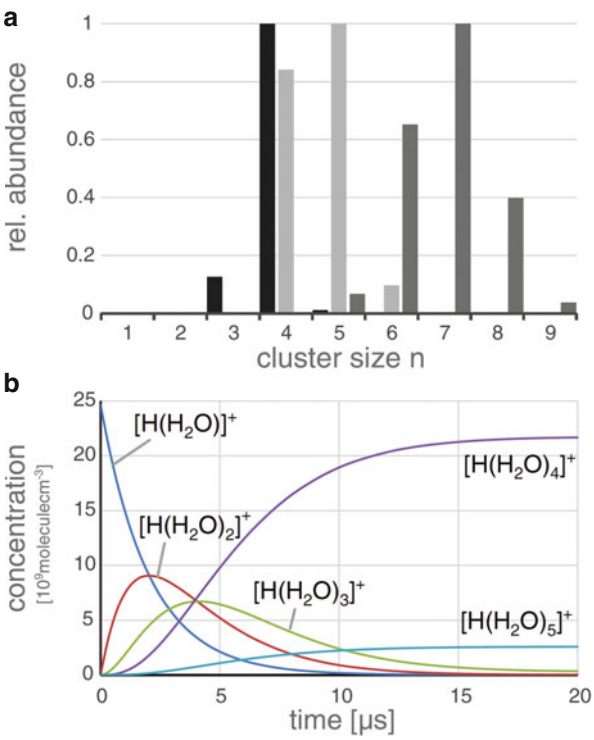

Fig. 7.23 (**a**) Bar graph representing the relative $[(H_2O)_n + H]^+$ cluster ion distribution for $n = 1$–9 in the presence of 1 ppm (v/v, *black*), 100 ppm (v/v, *light grey*), and 1 ‰ (v/v, *dark grey*) H_2O mixing ratio at 1000 mbar. (**b**) Temporal evolution of the concentrations of $[(H_2O)_n + H]^+$ cluster ions when starting H_3O^+ at a mixing ratio of 1 ppt as the only initial charged species present. Water background mixing ratio 10 ppm, $p =$ 1000 mbar. Clusters with $n =$ 6–9 are not discernible on this scale (Reproduced from Ref. [128] with permission. © Springer, 2014)

7.8.4 Negative-Ion Formation in APCI

All ionization processes known of NICI may occur in negative-ion formation in APCI, depending on the analyte. Oxygen is an important player as it easily forms $O_2^{-\bullet}$ reagent ions by electron capture [126, 127]:

$$O_2 + e^- \rightarrow O_2^{-\bullet} \tag{7.41}$$

These $O_2^{-\bullet}$ ions form adducts by association with the analyte M:

$$O_2^{-\bullet} + M \rightarrow [M + O_2]^{-\bullet} \tag{7.42}$$

Alternatively, negative molecular ions directly formed by electron capture can attach to molecular oxygen, thereby yielding the same product:

$$M^{-\bullet} + O_2 \rightarrow [M + O_2]^{-\bullet} \tag{7.43}$$

$[M + O_2]^{-\bullet}$ may either be detected as such or may dissociate to yield radical anions:

$$[M + O_2]^{-\bullet} \rightarrow M^{-\bullet} + O_2 \tag{7.44}$$

The latter dissociation requires $EA_M > EA_{O2}$, as oxygen would otherwise retain the electron.

The loss of a hydroperoxyl radical may lead to $[M - H]^-$ ions, i.e., proton abstraction, if the gas phase acidity of $[M - H]^-$ exceeds that of $HOO^\bullet$:

$$[M + O_2]^{-\bullet} \rightarrow [M - H]^- + HOO^\bullet \tag{7.45}$$

Halogenide ions can also play a role in analyte ion formation:

$$M + Hal^- \rightarrow [M + Hal]^- \tag{7.46}$$

Halogenide adducts can be observed when the analyte and/or a solvent are halogenated. Finally, adduct ion formation can occur with less abundant anions such as CO_3^-, NO_2^-, or OH^-.

7.8.5 APCI Spectra

The nature of the APCI plasma varies widely as both solvent and nebulizing gas contribute to the composition of the CI plasma, and thus, APCI spectra can resemble PICI, CTCI, NICI, or ECNI spectra depending on the actual conditions and ion polarity. The influence of solvent components, temperature, and other parameters explains why APCI conditions suffer from comparatively low reproducibility as compared to other ionization methods.

The heater cartridge typically operated at around 500 °C may lead to the impression of APCI as being a harsh ionization technique. However, the opposite is true. The softness of APCI even exceeds that of "classical" CI in the vacuum environment. The reasons for this apparent softness of APCI are numerous:

- The temperature of the aerosol droplets stays at the boiling temperature of the solvent until evaporation is complete. Thus, the temperature essentially remains below 70–100 °C and only rises to about 150–200 °C towards the exit of the heater cartridge.
- All excess energy of freshly formed analyte ions is effectively dissipated into the surrounding gas, because at atmospheric pressure, 10^6 ion–neutral collisions per millisecond guarantee immediate thermalization (Table 7.5) [128].
- Thermal energy at 150–200 °C is only about 0.1–0.2 eV, while bond breaking normally requires 2–3 eV.

- Decomposition rates at low internal energy are far too slow to permit a high amount of fragmentation within the few milliseconds between nebulization and entry into the interface.

APCI spectra are therefore characterized by no or at least a very moderate level of fragmentation.

The greatest advantage of APCI over ESI is that it actively generates ions from neutrals. Thus, APCI provides mass spectrometry with the means of applying low- to medium-polarity analytes eluting from a liquid chromatograph [130]. The use of APCI rapidly expanded in the mid-1990, perhaps because by then elaborate vacuum interfaces had become available from ESI technology. Nowadays, APCI is used where LC separation is required, but ESI is not applicable to the compound class of interest [130–133]. A set of typical APCI spectra is provided below.

Positive-ion APCI of triacylglycerols Liquid chromatographic separation of triacylglycerols from soybean oil delivered dozens of fats differing in type and combination of fatty acids. The positive-ion APCI mass spectra of two selected triacylglycerols, triolein (OOO) and 1(3)-palmitoyl-2-stearoyl-3(1)-linoleoyl glycerol (PSL), are shown in Fig. 7.24 [131]. The APCI spectra exhibit $[M+H]^+$ ions and fragment ions characteristic of fatty acid composition and – to a certain degree – of isomers. While triolein can only form one distinctive diacyl fragment $[OO]^+$, the other fat yields $[PS]^+$, $[PL]^+$, and $[LS]^+$ as primary fragment ions. The fatty acids themselves are also revealed by their acylium ions in the low-mass range.

Negative-ion APCI of chloro-nitrobenzofurazan derivatives Negative-ion APCI spectra of alkylamino derivatives of 4-chloro-7-nitrobenzofurazan (NBDCl) were measured from acetonitrile/methanol solution. While the *N*,*N*-dimethylamino derivative preferably forms the radical anion, $M^{-\bullet}$, *m*/*z* 208, the *N*-ethyl isomer prefers the $[M - H]^-$ ion, *m*/*z* 207. This major change in spectral appearance is due to the missing slightly acidic hydrogen in the NBDCl isomer with the tertiary amino group. This demonstrates the strong influence of analyte structure on negative-ion (AP)CI spectra (Fig. 7.25) [134, 135].

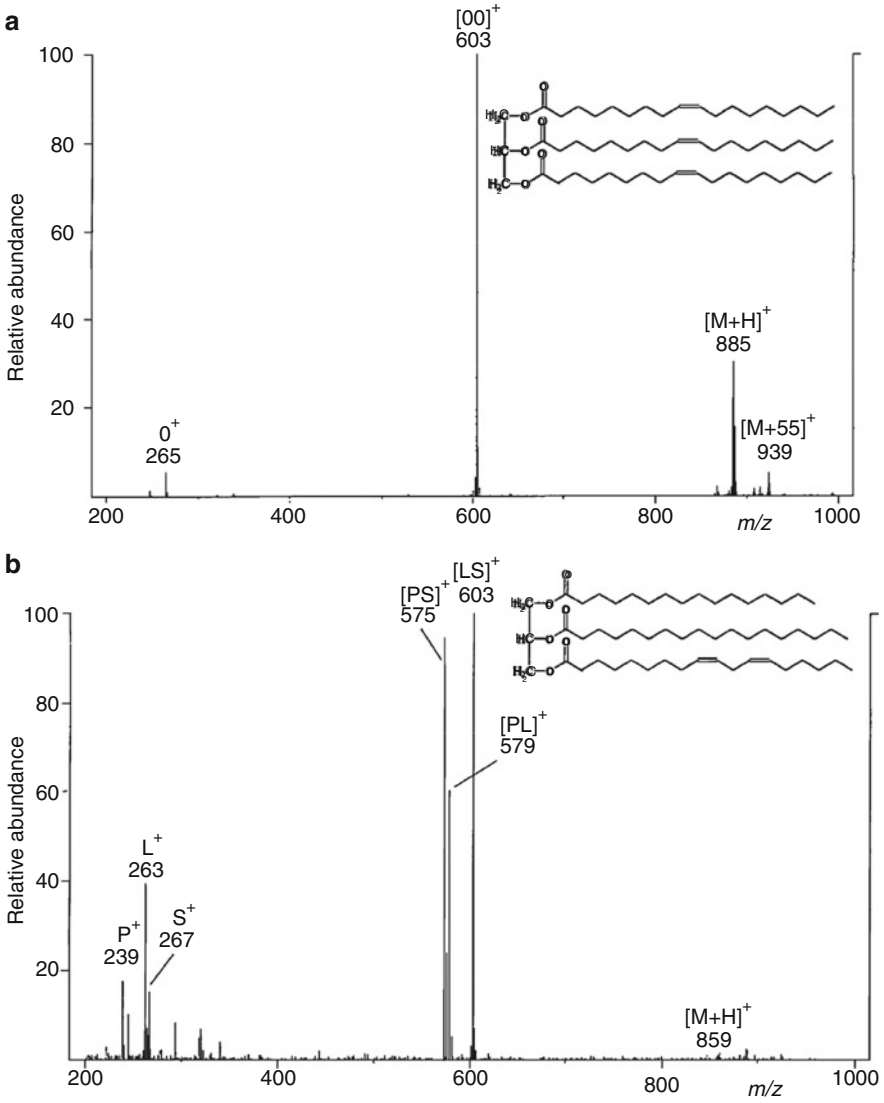

Fig. 7.24 Positive-ion APCI mass spectra of (**a**) triolein (OOO) and (**b**) 1(3)-palmitoyl-2-stearoyl-3 (1)-linoleoyl glycerol (PSL) from soybean oil. The $[M+55]^+$ ion in (**a**) is a solvent (proprionitrile) adduct (Reproduced from Ref. [131] with permission. © John Wiley & Sons, Ltd, 1997)

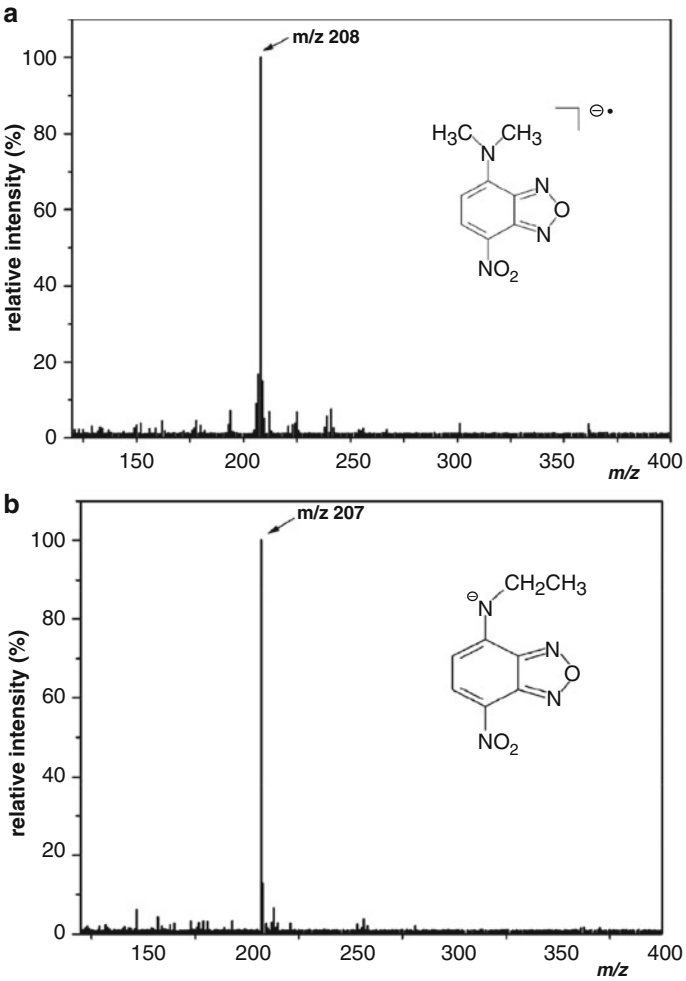

Fig. 7.25 Negative-ion APCI spectra of alkylamino derivatives of 4-chloro-7-nitrobenzofurazan (NBDCl). (**a**) The *N*,*N*-dimethylamino derivative preferably forms the radical anion, $M^{-\bullet}$, while (**b**) the *N*-ethyl form prefers the $[M–H]^-$ ion (Adapted from Ref. [135] with permission. © The Royal Society of Chemistry, 2002)

7.9 Atmospheric Pressure Photoionization

Atmospheric pressure photoionization (APPI) was introduced in 2000 [136] as a complement or alternative to APCI [130, 137, 138]. In APPI, a UV light source replaces the corona discharge-powered plasma, while the pneumatic sprayer and the heated vaporizer remain almost unaffected (Fig. 7.26) [139–141]. Apart from

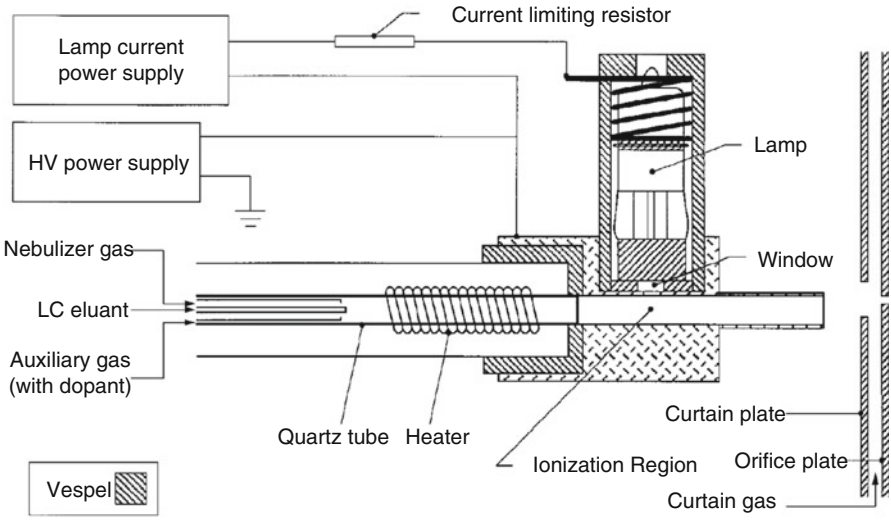

Fig. 7.26 APPI source comprising the heated nebulizer probe, photoionization UV lamp and mounting bracket (Reproduced from Ref. [136] by permission. © American Chemical Society, 2000)

the UV light, the most relevant modification is the use of a quartz tube to guide the hot vapor toward the sampling orifice. Quartz is required to transmit the UV light emitted by a noble gas discharge lamp.

Quick method switching
Modern instruments with atmospheric pressure ion sources are all constructed as to permit easy exchange of spray heads for rapid switching between ESI, APCI, and APPI [139, 142]. There is no interruption of instrument vacuum and mounting of spray heads takes just a minute, but there is a 10–15-min delay for APCI or APPI vaporizers to fully heat up for operation or to sufficiently cool down before removal is possible without risk of injury from hot parts.

7.9.1 Ion Formation in APPI

Statistically, the light emitted by the UV lamp will be absorbed by solvent molecules or eventually by nitrogen used for spraying, rather than by the analyte molecules. Therefore, the energy of the UV photons and the ionization energies of the compounds are decisive for the initiation of the APPI process (Fig. 7.27) [141]. In APPI, krypton lamps are commonly used as UV light source. In addition to the main emission of photons bearing 10.0 eV of energy there is a smaller fraction of photons of 10.6 eV. According to this energy level, krypton achieves ionization of most analytically relevant compounds while it blanks ionization of

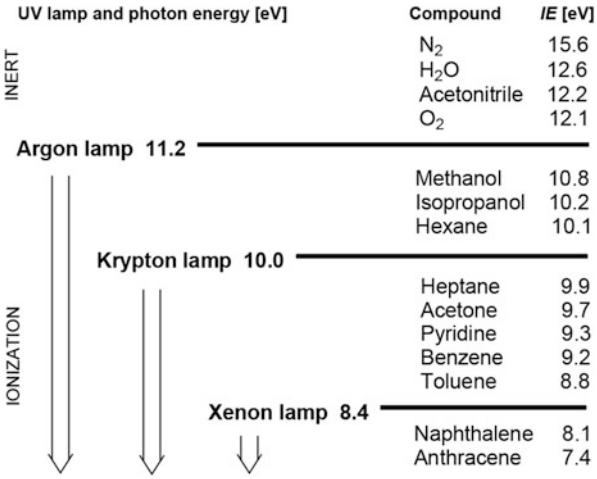

Fig. 7.27 Relationship between UV lamps and their photon energies used for APPI and ionization energies of typical compounds

some frequently used solvents and atmospheric gases [142]. APPI therefore has a higher compound class selectivity than APCI.

Provided the analyte, AB, has a UV chromophore, it can absorb the light to undergo *photoexcitation*, which merely delivers excited neutrals:

$$AB + h\nu \rightarrow AB^* \tag{7.47}$$

These electronically excited molecules AB* can either undergo radiative decay

$$AB^* \rightarrow AB + h\nu \tag{7.48}$$

or radiationless decay processes such as *photodissociation* to yield radicals

$$AB^* \rightarrow A^\bullet + B^\bullet \tag{7.49}$$

or *collisional quenching* with neutrals (N):

$$AB^* + N \rightarrow AB + N^* \tag{7.50}$$

More advantageous from the application point of view is *photoionization* (PI) of the analyte where AB* essentially represents a transition state:

$$AB + h\nu \rightarrow AB^* \rightarrow AB^{+\bullet} + e^- \tag{7.51}$$

However, photoionization of analyte molecules is neither energetically nor statistically a favored process [141]. Even if ions $AB^{+\bullet}$ have formed, they can be lost by neutralization via *recombination* with free electrons present in the plasma, eventually along with moderating ion–neutral collisions:

$$AB^{+\bullet} + e^- \rightarrow AB^* \tag{7.52}$$

$$AB^{+\bullet} + e^- + N \rightarrow AB + e^- + N \tag{7.52a}$$

Instead of relying on direct photoionization to occur, one normally would prefer a chemical ionization process where the reagent ions are formed by photoionization of a reagent gas. If the solvent (S) cannot be photoionized to play this role, a UV-absorbing dopant (D) may be added [136, 140, 143–146]. The dopant ions may then react with the analyte by *charge transfer*:

$$D^{+\bullet} + AB \rightarrow AB^{+\bullet} + D \tag{7.53}$$

Alternatively, dopant ions can lead to the formation of solvent reagent ions:

$$D^{+\bullet} + S \rightarrow [D - H]^{\bullet} + [S + H]^+ \tag{7.54}$$

These $[S+H]^+$ ions can finally protonate the analyte molecules [141, 142]:

$$[S + H]^+ + AB \rightarrow S + [AB + H]^+ \tag{7.55}$$

Methanol, for example, cannot be ionized by use of a krypton lamp, but addition of some acetone as dopant will allow the processes described in Eqs. 7.53, 7.54, and 7.55 to occur. Obviously, rich chemistry is involved until the neutral analyte has been transformed into $AB^{+\bullet}$ or $[AB+H]^+$ ions with sufficient efficiency [145, 146].

Negative-ion formation in APPI can occur by mechanisms analogous to APCI where electron capture by molecular oxygen initiates the cascade of reactions (Sect. 7.8.5).

More of CI than expected

Overall and in general, much of what happens in APPI bears close resemblance to APCI and CI, while the role of direct photoionization for analyte ion formation is less pronounced than suggested by its name.

7.9.2 APPI Spectra

The appearance of APPI spectra strongly depends on the actual combination of UV lamp, solvent, analyte, and eventually dopant. It is not always straightforward to predict whether protonation or molecular ion formation will dominate a positive-ion APPI spectrum, and analogously, whether deprotonation or radical anion formation will be observed in negative-ion mode. As a rule of thumb, molecules of higher

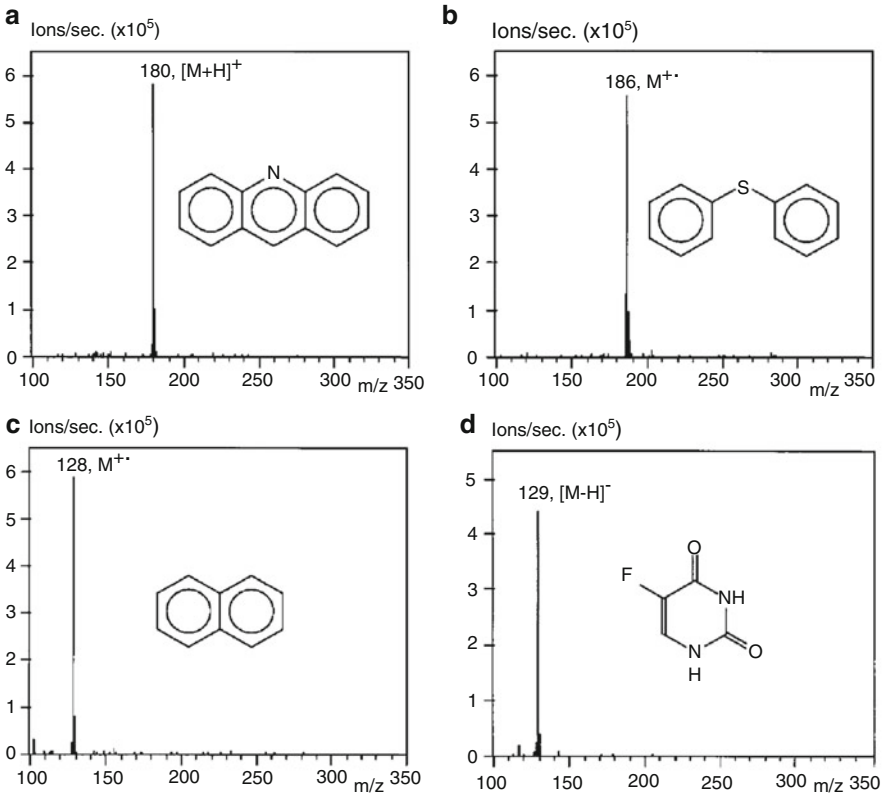

Fig. 7.28 Positive-ion APPI spectra of (**a**) acridine, (**b**) diphenyl sulfide, and (**c**) naphthalene showing how *PA* and *IE* of a compound affect ion formation. (**d**) Negative-ion APPI spectrum of 5-fluorouracil where the acidity of the imide is sufficient to form $[M–H]^-$ ions (Adapted from Ref. [136] with permission. © American Chemical Society, 2000)

proton affinity (*PA*) tend to form $[M+H]^+$ ions while nonpolar analytes, in particular those of low ionization energy (*IE*), preferably form $M^{+\bullet}$ ions [145]. In negative-ion mode, acidic molecules easily deliver $[M–H]^-$ ions, while those of high electron affinity (*EA*) undergo electron capture to yield $M^{-\bullet}$ ions. Unfortunately, APPI tends towards mixed ion formation, e.g., $M^{+\bullet}$ beside $[M+H]^+$ ions, the ratio of which is strongly influenced by the actual dopant [140, 143, 147, 148]. Like APCI, APPI often provides spectra showing almost exclusively ions representing the intact molecule. Some typical APPI spectra are compiled below (Fig. 7.28) [136].

One compound ionized by three methods Often, different soft ionization methods can be employed for the same compound with comparable success [149]. This does, however, not imply that each method is delivering the same type of analyte ion of a given compound. A comparison of positive-ion electrospray

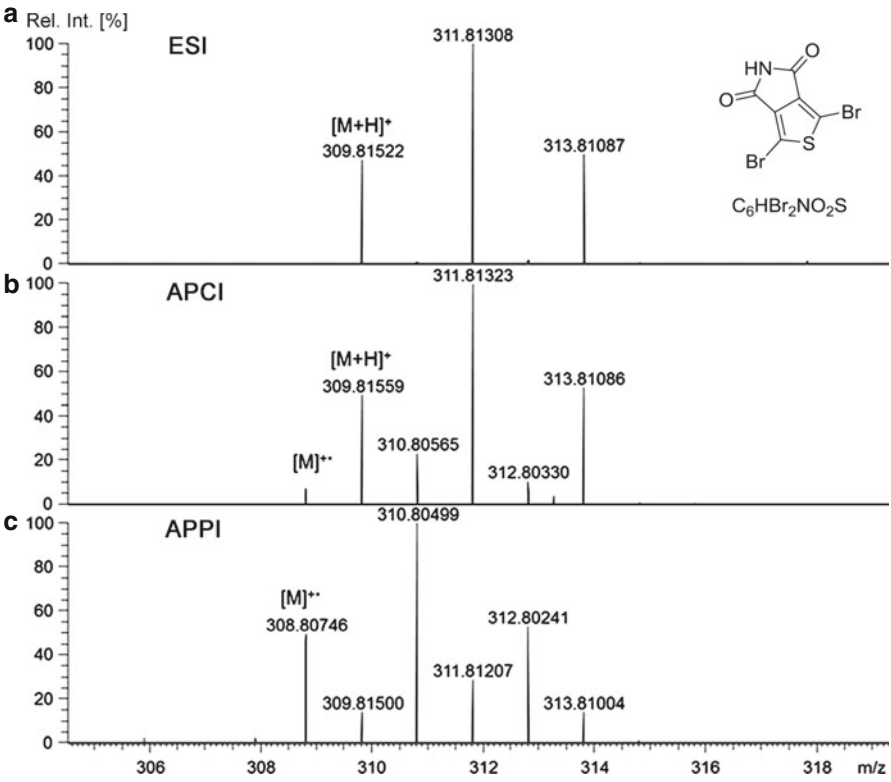

Fig. 7.29 Comparison of positive-ion (**a**) ESI, (**b**) APCI, and (**c**) APPI spectra of dibromothieno [3,4-*c*]pyrrole-4,6-dione. Note that there is also a small contribution of $M^{+\bullet}$ in APCI (Adapted from Ref. [148] by permission. © Wiley, 2014)

ionization (ESI, Chap. 12), APCI, and APPI spectra of dibromothieno[3,4-*c*]pyrrole-4,6-dione demonstrates this fact (Fig. 7.29) [148]. While ESI will exclusively deliver even-electron ions, both APCI and APPI may either result in formation of $[M+H]^+$ or $M^{+\bullet}$ ions depending on parameters such as ionization energy of the analyte and of the solvent as well as on their relative proton affinities.

Effect of different dopants In APPI, the formation of molecular ions, $M^{+\bullet}$, versus protonated molecules, $[M+H]^+$, also strongly depends on the type of dopant used [145, 146, 148]. A comparison of positive-ion APPI spectra of dibromothieno [3,4-*c*]pyrrole-4,6-dione as obtained using either chlorobenzene, bromobenzene, toluene, or no dopant exemplifies this effect (Fig. 7.30) [148].

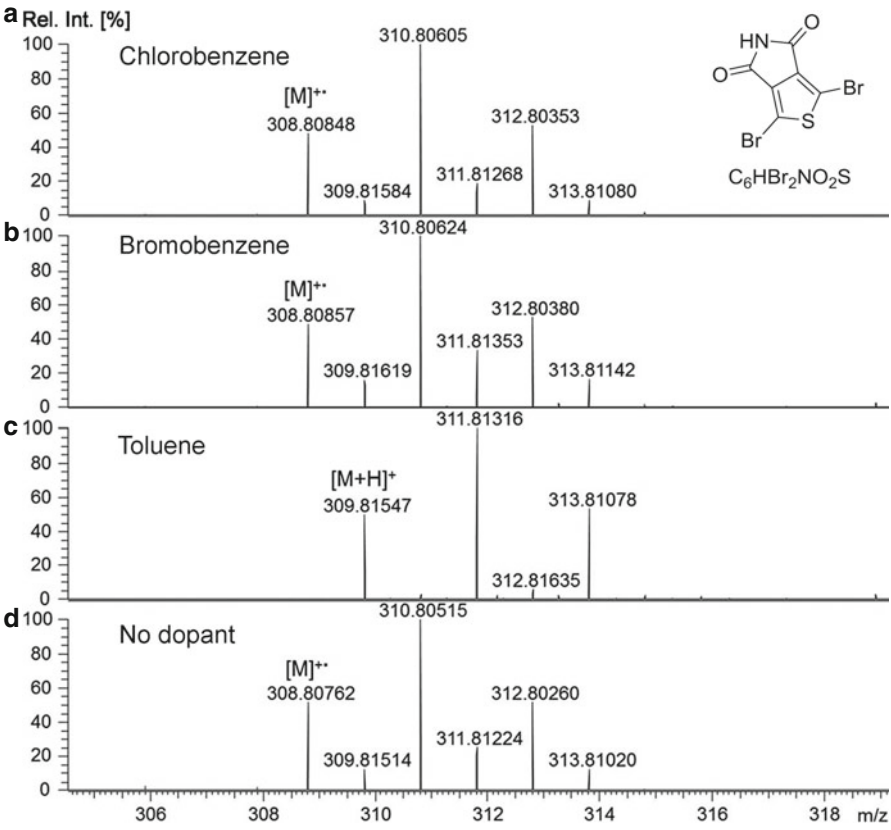

Fig. 7.30 Influence of dopants on positive-ion APPI spectra of dibromothieno[3,4-*c*]pyrrole-4,6-dione. The formation of $M^{+\bullet}$ versus $[M+H]^+$ ions depends on the actual dopant: (**a**) chlorobenzene, (**b**) bromobenzene, (**c**) toluene, and (**d**) no dopant (Adapted from Ref. [148] by permission. © Wiley, 2014)

Analyte supply from solution

Both APCI and APPI differ from vacuum CI in that the analyte is supplied from dilute solutions rather than by direct evaporation of liquids or solids from a probe or reservoir inlet. This does not only ensure the compatibility of APCI and APPI with liquid chromatography (Sect. 14.5) but also results in a softer transition from condensed phase to gas phase. Nonetheless, all CI methods involve gas phase ionization, and thus, require some evaporation to be performed prior to ionization as an integral part of the technique. All CI techniques are therefore perfectly compatible with gas chromatography (Sect. 14.4).

7.10 Overview of CI, APCI, and APPI

Common Features of Chemical Ionization Techniques
The term *chemical ionization* (CI) usually applies to all ionization processes that proceed via ion–molecule reactions. In CI, analyte molecules, M, are ionized by reacting with *reagent ions* generated in a foregoing process from a *reagent gas*. Classically, chemical ionization was performed on the microsecond-time scale in medium vacuum, typically at about 1 mbar (1 collision μs^{-1}). The occurrence of ion–molecule reactions is not restricted to the vacuum environment – on the contrary, rates of bimolecular reactions increase along with rising pressure. Performing chemical ionization on the millisecond-time scale and at atmospheric pressure (10^6 collisions ms^{-1}) thus improves ionization efficiency. Additionally, immediate thermalization of the freshly formed ions reduces fragmentation.

Fundamental Ionization Pathways
Chemical ionization proceeds either by transfer of an electron, proton, or other ions between the reactants. Positive-ion chemical ionization (PICI) comprises four fundamental pathways of ion formation from neutrals: proton transfer, electrophilic addition, anion abstraction, and charge transfer (CT). Negative-ion chemical ionization (NICI) either involves deprotonation, nucleophilic addition, or ion-pair formation. A fourth process observed along with NICI is electron capture (EC). However, electron capture negative ionization (ECNI) is not a chemical ionization process in the strict sense. These fundamental ionization pathways apply whether CI is performed in vacuum or at atmospheric pressure and independent of whether the primary step of reagent ion formation is initiated by energetic electrons (vacuum CI), a corona discharge (APCI), UV photons (APPI), or any other source.

Analytes
Whether an analyte is suitable to be analyzed by a CI technique depends on the type of particular CI process to be applied. Obviously, protonating PICI will be beneficial for other compounds than CTCI or ECNI. In general, most analytes accessible to electron ionization (EI, Sect. 5.6) can be analyzed by protonating PICI. PICI spectra are particularly useful as a complement to EI spectra when molecular ion peaks are absent or very weak in EI. CTCI and ECNI play a role where selectivity and/or very high sensitivity for a certain compound class is desired (Table 7.6). The typical mass range for vacuum CI reaches from 60 u (above reagent ions) to 1200 u. APCI and APPI are softer due to immediate thermalization of the ions, and thus, extend the upper range of ions representing the intact molecule to about 2000 u. APPI can deliver ions of less polar analytes than APCI.

Today, desorption chemical ionization (DCI) and particularly pyrolysis-DCI are rarely used because APCI, APPI, and many other soft ionization methods, especially those combining desorption and ionization (Chaps. 8, 10, 11, 12, and 13) offer more promising and more convenient ways of mass spectral analysis. Nonetheless, there are exceptions when materials such as resins, varnishes, rubbers, and others of similar complexity are to be studied.

Table 7.6 Chemical ionization for different groups of analytes

Analyte	Thermodynamic properties[a]	Example	Suggested CI pathway
Low polarity, no heteroatoms	Low to high *IE*, low *PA*, low *EA*	Alkanes, alkenes, aromatic hydrocarbons	CTCI
Low to medium polarity, one or two heteroatoms	Low to medium *IE*, medium to high *PA*, low *EA*	Alcohols, amines, esters, heterocyclic compounds	PICI, CTCI
Medium to high polarity, some heteroatoms	Low to medium *IE*, high *PA* and low *EA*	Diols, triols, amino acids, disaccharides, substituted aromatic or heterocyclic compounds	PICI
Low to high polarity, halogens (especially F or Cl)	Medium *IE*, low *PA*, medium to high *EA*	Halogenated and nitrocompounds, derivatives, e.g., trifluoroacetate, pentafluorobenzyl	ECNI
High polarity, medium to high molecular mass	Low to medium *IE*, high *PA* and low *EA*	Mono- to tetrasaccharides, other polar oligomers, complex materials	DCI
High polarity, very high molecular mass	Decomposition products of low to medium *IE*, high *PA* and low *EA*	humic compounds, synthetic polymers, complex materials	Py-DCI

[a]*IE* ionization energy, *PA* proton affinity, *EA* electron affinity

Table 7.7 Ions formed by chemical ionization techniques

Analytes	Positive ions	Negative ions
Nonpolar	$M^{+\bullet}$	$M^{-\bullet}$
Medium polarity	$M^{+\bullet}$ and/or $[M+H]^+$, $[M+cat]^{+a}$,{*clusters* $[2M]^{+\bullet}$ and/or $[2M+H]^+$, $[2M+cat]^{+a}$}[b]	$M^{-\bullet}$ and/or $[M-H]^-$, $[M+an]^{-a}${*clusters* $[2M]^{-\bullet}$ and/or $[2M-H]^-$, $[2M+an]^{-a}$}[b]
Polar	$[M+H]^+$, $[M+cat]^{+a}$,{*clusters* $[2M+H]^+$, $[2M+cat]^{+a}$ }[b]	$[M-H]^-$, $[M+an]^{-a}${*clusters* $[2M-H]^-$, $[2M+an]^{-a}$}[b]

[a]Cation cat^+ and anion an^-
[b]Braces denote occasionally accompanying species

Ions Formed

The various options for selecting pathways of ion formation and the variety of available CI methods result in a comparatively large number of different types of analyte ions that can occur. The chiefly occurring type of analyte ions strongly depends on such general parameters as mass, polarity, volatility, and intrinsic properties like ionization energy, proton affinity, or electron affinity. And then, the selection of either positive-ion or negative-ion mode creates a different set of analyte ions. Table 7.7 provides a basic classification.

Relationship to Other Ionization Techniques

Reaction sequences analogous to *atmospheric pressure chemical ionization* (APCI) do occur whenever ionization is performed in an atmosphere with traces of water, e.g., *direct analysis in real time* (DART, Sect. 13.8).

References

1. Talrose VL, Ljubimova AK (1998) Secondary Processes in the Ion Source of a Mass Spectrometer (Presented by Academician N.N. Semenov 27 Viii 1952) – Reprinted from Report of the Soviet Academy of Sciences, Vol LXXXVI, -N5 (1952). J Mass Spectrom 33:502–504
2. Munson MSB, Field FH (1965) Reactions of Gaseous Ions. XV. Methane + 1% Ethane and Methane + 1% Propane. J Am Chem Soc 87:3294–3299. doi:10.1021/ja01093a002
3. Munson MSB (1965) Proton Affinities and the Methyl Inductive Effect. J Am Chem Soc 87:2332–2336. doi:10.1021/ja01089a005
4. Munson MSB, Field FH (1966) Chemical Ionization Mass Spectrometry. I General Introduction. J Am Chem Soc 88:2621–2630. doi:10.1021/ja00964a001
5. Munson MSB (2000) Development of Chemical Ionization Mass Spectrometry. Int J Mass Spectrom 200:243–251. doi:10.1016/S1387-3806(00)00301-8
6. Richter WJ, Schwarz H (1978) Chemical Ionization – A Highly Important Productive Mass Spectrometric Analysis Method. Angew Chem 90:449–469. doi:10.1002/anie.197804241
7. Harrison AG (1992) Chemical Ionization Mass Spectrometry. CRC Press, Boca Raton
8. Todd JFJ (1995) Recommendations for Nomenclature and Symbolism for Mass Spectroscopy Including an Appendix of Terms Used in Vacuum Technology. Int J Mass Spectrom Ion Proc 142:211–240. doi:10.1016/0168-1176(95)93811-F
9. Sparkman OD (2006) Mass Spectrometry Desk Reference. Global View Publishing, Pittsburgh
10. Murray KK, Boyd RK, Eberlin MN, Langley GJ, Li L, Naito Y (2013) Definitions of Terms Relating to Mass Spectrometry (IUPAC Recommendations 2013). Pure Appl Chem 85:1515–1609. doi:10.1351/PAC-REC-06-04-06
11. Griffith KS, Gellene GI (1993) A Simple Method for Estimating Effective Ion Source Residence Time. J Am Soc Mass Spectrom 4:787–791. doi:10.1016/1044-0305(93)80036-X
12. Field FH, Munson MSB (1965) Reactions of Gaseous Ions. XIV. Mass Spectrometric Studies of Methane at Pressures to 2 Torr. J Am Chem Soc 87:3289–3294. doi:10.1021/ja01093a001
13. Hunt DF, Ryan JFI (1971) Chemical Ionization Mass Spectrometry Studies. I. Identification of Alcohols. Tetrahedron Lett 12:4535–4538. doi:10.1016/S0040-4039(01)97523-9
14. Herman JA, Harrison AG (1981) Effect of Reaction Exothermicity on the Proton Transfer Chemical Ionization Mass Spectra of Isomeric C_5 and C_6 Alkanols. Can J Chem 59:2125–2132. doi:10.1139/v81-307
15. Beggs D, Vestal ML, Fales HM, Milne GWA (1971) Chemical Ionization Mass Spectrometer Source. Rev Sci Inst 42:1578–1584. doi:10.1063/1.1684943
16. Schröder E (1991) Massenspektrometrie – Begriffe und Definitionen. Springer-Verlag, Heidelberg
17. Ghaderi S, Kulkarni PS, Ledford EB Jr, Wilkins CL, Gross ML (1981) Chemical Ionization in Fourier Transform Mass Spectrometry. Anal Chem 53:428–437. doi:10.1021/ac00226a011
18. Price P (1991) Standard Definitions of Terms Relating to Mass Spectrometry. A Report from the Committee on Measurements and Standards of the Amercian Society for Mass Spectrometry. J Am Soc Mass Spectrom 2:336–348. doi:10.1016/1044-0305(91)80025-3
19. Heck AJR, de Koning LJ, Nibbering NMM (1991) Structure of Protonated Methane. J Am Soc Mass Spectrom 2:454–458. doi:10.1016/1044-0305(91)80030-B

20. Mackay GI, Schiff HI, Bohme KD (1981) A Room-Temperature Study of the Kinetics and Energetics for the Protonation of Ethane. Can J Chem 59:1771–1778. doi:10.1139/v81-265
21. Fisher JJ, Koyanagi GK, McMahon TB (2000) The $C_2H_7^+$ Potential Energy Surface: A Fourier Transform Ion Cyclotron Resonance Investigation of the Reaction of Methyl Cation with Methane. Int J Mass Spectrom 195(196):491–505. doi:10.1016/S1387-3806(99)00231-6
22. Drabner G, Poppe A, Budzikiewicz H (1990) The Composition of the Methane Plasma. Int J Mass Spectrom Ion Proc 97:1–33. doi:10.1016/0168-1176(90)85037-3
23. Thompson KC, Crittenden DL, Jordan MJT (2005) $CH_5^{+\cdot}$: Chemistry's Chameleon Unmasked. J Am Chem Soc 127:4954–4958. doi:10.1021/ja0482280
24. Heck AJR, de Koning LJ, Nibbering NMM (1991) On the Structure and Unimolecular Chemistry of Protonated Halomethanes. Int J Mass Spectrom Ion Proc 109:209–225. doi:10.1016/0168-1176(91)85105-U
25. Herman JA, Harrison AG (1981) Effect of Protonation Exothermicity on the Chemical Ionization Mass Spectra of Some Alkylbenzenes. Org Mass Spectrom 16:423–427. doi:10.1002/oms.1210161002
26. Munson MSB, Field FH (1965) Reactions of Gaseous Ions. XVI Effects of Additives on Ionic Reactions in Methane. J Am Chem Soc 87:4242–4247. doi:10.1021/ja00947a005
27. Kuck D, Petersen A, Fastabend U (1998) Mobile Protons in Large Gaseous Alkylbenzenium Ions. The 21-Proton Equilibration in Protonated Tetrabenzylmethane and Related "Proton Dances". Int J Mass Spectrom 179(180):129–146. doi:10.1016/S1387-3806(98)14168-4
28. Kuck D (2002) Half a Century of Scrambling in Organic Ions: Complete, Incomplete, Progressive and Composite Atom Interchange. Int J Mass Spectrom 213:101–144. doi:10.1016/S1387-3806(01)00533-4
29. Fales HM, Milne GWA, Axenrod T (1970) Identification of Barbiturates by Chemical Ionization Mass Spectrometry. Anal Chem 42:1432–1435. doi:10.1021/ac60294a040
30. Milne GWA, Axenrod T, Fales HM (1970) Chemical Ionization Mass Spectrometry of Complex Molecules. IV Amino Acids. J Am Chem Soc 92:5170–5175. doi:10.1021/ja00720a029
31. Fales HM, Milne GWA (1970) Chemical Ionization Mass Spectrometry of Complex Molecules. II Alkaloids. J Am Chem Soc 92:1590–1597. doi:10.1021/ja00709a028
32. Herman JA, Harrison AG (1981) Energetics and Structural Effects in the Fragmentation of Protonated Esters in the Gas Phase. Can J Chem 59:2133–2145. doi:10.1139/v81-308
33. Milne GWA, Fales HM, Axenrod T (1970) Identification of Dangerous Drugs by Isobutane Chemical Ionization Mass Spectrometry. Anal Chem 42:1815–1820. doi:10.1021/ac60307a048
34. Takeda N, Harada KI, Suzuki M, Tatematsu A, Kubodera T (1982) Application of Emitter Chemical Ionization Mass Spectrometry to Structural Characterization of Aminoglycoside Antibiotics. Org Mass Spectrom 17:247–252. doi:10.1002/oms.1210170602
35. McGuire JM, Munson B (1985) Comparison of Isopentane and Isobutane as Chemical Ionization Reagent Gases. Anal Chem 57:680–683. doi:10.1021/ac00280a024
36. McCamish M, Allan AR, Roboz J (1987) Poly(dimethylsiloxane) as Mass Reference for Accurate Mass Determination in Isobutane Chemical Ionization Mass Spectrometry. Rapid Commun Mass Spectrom 1:124–125. doi:10.1002/rcm.1290010711
37. Maeder H, Gunzelmann KH (1988) Straight-Chain Alkanes As Reference Compounds for Accurate Mass Determination in Isobutane Chemical Ionization Mass Spectrometry. Rapid Commun Mass Spectrom 2:199–200. doi:10.1002/rcm.1290021003
38. Hunt DF, McEwen CN, Upham RA (1971) Chemical Ionization Mass Spectrometry. II. Differentiation of Primary, Secondary, and Tertiary Amines. Tetrahedron Lett 12:4539–4542. doi:10.1016/S0040-4039(01)97524-0
39. Busker E, Budzikiewicz H (1979) Studies in Chemical Ionization Mass Spectrometry. 2. Isobutane and Nitric Oxide Spectra of Alkynes. Org Mass Spectrom 14:222–226. doi:10.1002/oms.1210140412

40. Keough T, DeStefano AJ (1981) Factors Affecting Reactivity in Ammonia Chemical-Ionization Spectrometry. Org Mass Spectrom 16:527–533. doi:10.1002/oms.1210161205
41. Hancock RA, Hodges MG (1983) A Simple Kinetic Method for Determining Ion-Source Pressures for Ammonia CIMS. Int J Mass Spectrom Ion Phys 46:329–332. doi:10.1016/0020-7381(83)80119-3
42. Rudewicz P, Munson B (1986) Effect of Ammonia Partial Pressure on the Sensitivities for Oxygenated Compounds in Ammonia Chemical Ionization Mass Spectrometry. Anal Chem 58:2903–2907. doi:10.1021/ac00127a003
43. Lawrence DL (1990) Accurate Mass Measurement of Positive Ions Produced by Ammonia Chemical Ionization. Rapid Commun Mass Spectrom 4:546–549. doi:10.1002/rcm.1290041216
44. Brinded KA, Tiller PR, Lane SJ (1993) Triton X-100 As a Reference Compound for Ammonia High-Resolution Chemical Ionization Mass Spectrometry and as a Tuning and Calibration Compound for Thermospray. Rapid Commun Mass Spectrom 7:1059–1061. doi:10.1002/rcm.1290071119
45. Wu HF, Lin YP (1999) Determination of the Sensitivity of an External Source Ion Trap Tandem Mass Spectrometer Using Dimethyl Ether Chemical Ionization. J Mass Spectrom 34:1283–1285. doi:10.1002/(SICI)1096-9888(199912)34:12<1283::AID-JMS900>3.0.CO;2-M
46. Barry R, Munson B (1987) Selective Reagents in Chemical Ionization Mass Spectrometry: Diisopropyl Ether. Anal Chem 59:466–471. doi:10.1021/ac00130a019
47. Allgood C, Lin Y, Ma YC, Munson B (1990) Benzene as a Selective Chemical Ionization Reagent Gas. Org Mass Spectrom 25:497–502. doi:10.1002/oms.1210251003
48. Srinivas R, Vairamani M, Mathews CK (1993) Gase-Phase Halo Alkylation of C_{60}-Fullerene by Ion-Molecule Reaction Under Chemical Ionization. J Am Soc Mass Spectrom 4:894–897. doi:10.1016/1044-0305(93)87007-Y
49. Budzikiewicz H, Blech S, Schneider B (1991) Studies in Chemical Ionization. XXVI. Investigation of Aliphatic Dienes by Chemical Ionization with Nitric Oxide. Org Mass Spectrom 26:1057–1060. doi:10.1002/oms.1210261205
50. Schneider B, Budzikiewicz H (1990) A Facile Method for the Localization of a Double Bond in Aliphatic Compounds. Rapid Commun Mass Spectrom 4:550–551. doi:10.1002/rcm.1290041217
51. Fordham PJ, Chamot-Rooke J, Guidice E, Tortajada J, Morizur JP (1999) Analysis of Alkenes by Copper Ion Chemical Ionization Gas Chromatography/Mass Spectrometry and Gas Chromatography/Tandem Mass Spectrometry. J Mass Spectrom 34:1007–1017. doi:10.1002/(SICI)1096-9888(199910)34:10<1007::AID-JMS854>3.0.CO;2-E
52. Peake DA, Gross ML (1985) Iron(I) Chemical Ionization and Tandem Mass Spectrometry for Locating Double Bonds. Anal Chem 57:115–120. doi:10.1021/ac00279a031
53. Lindinger W, Jordan A (1998) Proton-Transfer-Reaction Mass Spectrometry (PTR-MS): Online Monitoring of Volatile Organic Compounds at pptv Levels. Chem Soc Rev 27:347–354. doi:10.1039/a827347z
54. Lindinger W, Hansel A, Jordan A (1998) Online Monitoring of Volatile Organic Compounds at pptv Levels by Means of Proton-Transfer-Reaction Mass Spectrometry (PTR-MS). Medical Applications, Food Control and Environmental Research. Int J Mass Spectrom Ion Proc 173:191–241. doi:10.1016/S0168-1176(97)00281-4
55. Blake RS, Monks PS, Ellis AM (2009) Proton-Transfer Reaction Mass Spectrometry. Chem Rev 109:861–896. doi:10.1021/cr800364q
56. de Gouw J, Warneke C (2007) Measurements of Volatile Organic Compounds in the Earth's Atmosphere Using Proton-Transfer-Reaction Mass Spectrometry. Mass Spectrom Rev 26:223–257. doi:10.1002/mas.20119
57. Fay LB, Yeretzian C, Blank I (2001) Novel Mass Spectrometry Methods in Flavour Analysis. Chimia 55:429–434

58. Sulzer P, Hartungen E, Hanel G, Feil S, Winkler K, Mutschlechner P, Haidacher S, Schottkowsky R, Gunsch D, Seehauser H, Striednig M, Juerschik S, Breiev K, Lanza M, Herbig J, Maerk L, Maerk TD, Jordan A (2014) A Proton Transfer Reaction-Quadrupole Interface Time-of-Flight Mass Spectrometer (PTR-QiTOF): High Speed Due to Extreme Sensitivity. Int J Mass Spectrom 368:1–5. doi:10.1016/j.ijms.2014.05.004
59. Edtbauer A, Hartungen E, Jordan A, Hanel G, Herbig J, Juerschik S, Lanza M, Breiev K, Maerk L, Sulzer P (2014) Theory and Practical Examples of the Quantification of CH_4, CO, O_2, and CO_2 with an Advanced Proton-Transfer-Reaction/Selective-Reagent-Ionization Instrument (PTR/SRI-MS). Int J Mass Spectrom 365-366:10–14. doi:10.1016/j.ijms.2013.11.014
60. Karl T, Guenther A, Yokelson RJ, Greenberg J, Potosnak M, Blake DR, Artaxo P (2007) The Tropical Forest and Fire Emissions Experiment: Emission, Chemistry, and Transport of Biogenic Volatile Organic Compounds in the Lower Atmosphere Over Amazonia. J Geophys Res Atmos 112:D18302-1–D18302/17. doi: 10.1029/2007JD008539
61. Hsu CS, Qian K (1993) Carbon Disulfide Charge Exchange as a Low-Energy Ionization Technique for Hydrocarbon Characterization. Anal Chem 65:767–771. doi:10.1021/ac00054a020
62. Einolf N, Munson B (1972) High-Pressure Charge Exchange Mass Spectrometry. Int J Mass Spectrom Ion Phys 9:141–160. doi:10.1016/0020-7381(72)80040-8
63. Allgood C, Ma YC, Munson B (1991) Quantitation Using Benzene in Gas Chromatography/Chemical Ionization Mass Spectrometry. Anal Chem 63:721–725. doi:10.1021/ac00007a014
64. Subba Rao SC, Fenselau C (1978) Evaluation of Benzene as a Charge Exchange Reagent. Anal Chem 50:511–515. doi:10.1021/ac50025a036
65. Sieck LW (1983) Determination of Molecular Weight Distribution of Aromatic Components in Petroleum Products by Chemical Ionization Mass Spectrometry with Chlorobenzene as Reagent Gas. Anal Chem 55:38–41. doi:10.1021/ac00252a013
66. Li YH, Herman JA, Harrison AG (1981) Charge Exchange Mass Spectra of Some C_5H_{10} Isomers. Can J Chem 59:1753–1759. doi:10.1139/v81-263
67. Abbatt JA, Harrison AG (1986) Low-Energy Mass Spectra of Some Aliphatic Ketones. Org Mass Spectrom 21:557–563. doi:10.1002/oms.1210210906
68. Herman JA, Li YH, Harrison AG (1982) Energy Dependence of the Fragmentation of Some Isomeric $C_6H_{12}^{+\cdot}$ Ions. Org Mass Spectrom 17:143–150. doi:10.1002/oms.1210170309
69. Chai R, Harrison AG (1981) Location of Double Bonds by Chemical Ionization Mass Spectrometry. Anal Chem 53:34–37. doi:10.1021/ac00224a010
70. Keough T, Mihelich ED, Eickhoff DJ (1984) Differentiation of Monoepoxide Isomers of Polyunsaturated Fatty Acids and Fatty Acid Esters by Low-Energy Charge Exchange Mass Spectrometry. Anal Chem 56:1849–1852. doi:10.1021/ac00275a021
71. Polley CW Jr, Munson B (1983) Nitrous Oxide As Reagent Gas for Positive Ion Chemical Ionization Mass Spectrometry. Anal Chem 55:754–757. doi:10.1021/ac00255a037
72. Harrison AG, Lin MS (1984) Stereochemical Applications of Mass Spectrometry. 3. Energy Dependence of the Fragmentation of Stereoisomeric Methylcyclohexanols. Org Mass Spectrom 19:67–71. doi:10.1002/oms.1210190204
73. Hsu CS, Cooks RG (1976) Charge Exchange Mass Spectrometry at High Energy. Org Mass Spectrom 11:975–983. doi:10.1002/oms.1210110909
74. Roussis S (1999) Exhaustive Determination of Hydrocarbon Compound Type Distributions by High Resolution Mass Spectrometry. Rapid Commun Mass Spectrom 13:1031–1051. doi:10.1002/(SICI)1097-0231(19990615)13:11<1031::AID-RCM602>3.0.CO;2-8
75. Hunt DF, Stafford GC Jr, Crow FW (1976) Pulsed Positive- and Negative-Ion Chemical Ionization Mass Spectrometry. Anal Chem 48:2098–2104. doi:10.1021/ac50008a014
76. von Ardenne M, Steinfelder K, Tümmler R (1971) Elektronenanlagerungs-Massenspektrographie Organischer Substanzen. Springer, Heidelberg

77. Dougherty RC, Weisenberger CR (1968) Negative Ion Mass Spectra of Benzene, Naphthalene, and Anthracene. A New Technique for Obtaining Relatively Intense and Reproducible Negative Ion Mass Spectra. J Am Chem Soc 90:6570–6571. doi:10.1021/ja01025a090
78. Dillard JG (1973) Negative Ion Mass Spectrometry. Chem Rev 73:589–644. doi:10.1021/cr60286a002
79. Bouma WJ, Jennings KR (1981) Negative Chemical Ionization Mass Spectrometry of Explosives. Org Mass Spectrom 16:330–335. doi:10.1002/oms.1210160802
80. Budzikiewicz H (1986) Studies in Negative Ion Mass Spectrometry. XI. Negative Chemical Ionization (NCI) of Organic Compounds. Mass Spectrom Rev 5:345–380. doi:10.1002/mas.1280050402
81. Kurvinen JP, Mu H, Kallio H, Xu X, Hoy CE (2001) Regioisomers of Octanoic Acid-Containing Structured Triacylglycerols Analyzed by Tandem Mass Spectrometry Using Ammonia Negative Ion Chemical Ionization. Lipids 36:1377–1382. doi:10.1007/s11745-001-0855-9
82. Gross JH (2009) Mass Spectrometry. In: Andrews DL (ed) Encyclopedia of Applied Spectroscopy. Wiley-VCH, Weinheim
83. Hunt DF, Crow FW (1978) Electron Capture Negative Ion Chemical Ionization Mass Spectrometry. Anal Chem 50:1781–1784. doi:10.1021/ac50035a017
84. Ong VS, Hites RA (1994) Electron Capture Mass Spectrometry of Organic Environmental Contaminants. Mass Spectrom Rev 13:259–283. doi:10.1002/mas.1280130305
85. Oehme M (1994) Quantification of Fg-Pg Amounts by Electron Capture Negative Ion Mass Spectrometry – Parameter Optimization and Practical Advice. Fresenius J Anal Chem 350:544–554. doi:10.1007/BF00321803
86. Bartels MJ (1994) Quantitation of the Tetrachloroethylene Metabolite *N*-Acetyl-*S*-(Trichlorovinyl)Cysteine in Rat Urine Via Negative Ion Chemical Ionization Gas Chromatography/Tandem Mass Spectrometry. Biol Mass Spectrom 23:689–694. doi:10.1002/bms.1200231107
87. Fowler B (2000) The Determination of Toxaphene in Environmental Samples by Negative Ion Electron Capture High Resolution Mass Spectrometry. Chemosphere 41:487–492. doi:10.1016/S0045-6535(99)00476-2
88. Laramée JA, Arbogast BC, Deinzer ML (1986) Electron Capture Negative Ion Chemical Ionization Mass Spectrometry of 1,2,3,4-Tetrachlorodibenzo-*p*-dioxin. Anal Chem 58:2907–2912. doi:10.1021/ac00127a004
89. Budzikiewicz H (1981) Mass Spectrometry of Negative Ions. 3. Mass Spectrometry of Negative Organic Ions. Angew Chem 93:635–649. doi:10.1002/anie.198106241
90. Bowie JH (1984) The Formation and Fragmentation of Negative Ions Derived from Organic Molecules. Mass Spectrom Rev 3:161–207. doi:10.1002/mas.1280030202
91. Stemmler EA, Hites RA (1988) The Fragmentation of Negative Ions Generated by Electron Capture Negative Ion Mass Spectrometry: A Review with New Data. Biomed Environ Mass Spectrom 17:311–328. doi:10.1002/bms.1200170415
92. Jensen KR, Voorhees KJ (2015) Analytical Applications of Electron Monochromator-Mass Spectrometry. Mass Spectrom Rev 34:24–42. doi:10.1002/mas.21395
93. Buchanan MV, Olerich G (1984) Differentiation of Polycyclic Aromatic Hydrocarbons Using Electron Capture Negative Chemical Ionization. Org Mass Spectrom 19:486–489. doi:10.1002/oms.1210191005
94. Oehme M (1983) Determination of Isomeric Polycyclic Aromatic Hydrocarbons in Air Particulate Matter by High-Resolution Gas Chromatography/Negative Ion Chemical Ionization Mass Spectrometry. Anal Chem 55:2290–2295. doi:10.1021/ac00264a021
95. Giese RW (1997) Detection of DNA Adducts by Electron Capture Mass Spectrometry. Chem Res Toxicol 10:255–270. doi:10.1021/tx9601263
96. Laramée JA, Mazurkiewicz P, Berkout V, Deinzer ML (1996) Electron Monochromator-Mass Spectrometer Instrument for Negative Ion Analysis of Electronegative Compounds.

Mass Spectrom Rev 15:15–42. doi:10.1002/(SICI)1098-2787(1996)15:1<15::AID-MAS2>3.0.CO;2-E
97. NIST webbook. http://webbook.nist.gov/
98. Williamson DH, Knighton WB, Grimsrud EP (2000) Effect of Buffer Gas Alterations on the Thermal Electron Attachment and Detachment Reactions of Azulene by Pulsed High Pressure Mass Spectrometry. Int J Mass Spectrom 195(196):481–489. doi:10.1016/S1387-3806(99)00142-6
99. Wei J, Liu S, Fedoreyev SA, Vionov VG (2000) A Study of Resonance Electron Capture Ionization on a Quadrupole Tandem Mass Spectrometer. Rapid Commun Mass Spectrom 14:1689–1694. doi:10.1002/1097-0231(20000930)14:18<1689::AID-RCM75>3.0.CO;2-G
100. Carette M, Zerega Y, Perrier P, Andre J, March RE (2000) Rydberg Electron-Capture Mass Spectrometry of 1,2,3,4-Tetrachlorodibenzo-*p*-Dioxin. Eur Mass Spectrom 6:405–408. doi:10.1255/ejms.362
101. Zerega Y, Carette M, Perrier P, Andre J (2002) Rydberg Electron Capture Mass Spectrometry of Organic Pollutants. Organohal Comp 55:151–154
102. Bendig P, Maier L, Lehnert K, Knapp H, Vetter W (2013) Mass Spectra of Methyl Esters of Brominated Fatty Acids and Their Presence in Soft Drinks and Cocktail Syrups. Rapid Commun Mass Spectrom 27:1083–1089. doi:10.1002/rcm.6543
103. Jenske R, Vetter W (2008) Gas Chromatography/Electron-Capture Negative Ion Mass Spectrometry for the Quantitative Determination of 2- and 3-Hydroxy Fatty Acids in Bovine Milk Fat. J Agric Food Chem 56:5500–5505. doi:10.1021/jf800647w
104. Yinon J (1982) Mass Spectrometry of Explosives: Nitro Compounds, Nitrate Esters, and Nitramines. Mass Spectrom Rev 1:257–307. doi:10.1002/mas.1280010304
105. Cappiello A, Famiglini G, Lombardozzi A, Massari A, Vadalà GG (1996) Electron Capture Ionization of Explosives with a Microflow Rate Particle Beam Interface. J Am Soc Mass Spectrom 7:753–758. doi:10.1016/1044-0305(96)00015-3
106. Knighton WB, Grimsrud EP (1995) High-Pressure Electron Capture Mass Spectrometry. Mass Spectrom Rev 14:327–343. doi:10.1002/mas.1280140406
107. Aubert C, Rontani J-F (2000) Perfluoroalkyl Ketones: Novel Derivatization Products for the Sensitive Determination of Fatty Acids by Gas Chromatography/Mass Spectrometry in Electron Impact and Negative Chemical Ionization Modes. Rapid Commun Mass Spectrom 14:960–966. doi:10.1002/(SICI)1097-0231(20000615)14:11<960::AID-RCM972>3.3.CO;2-R
108. Kato Y, Okada S, Atobe K, Endo T, Haraguchi K (2012) Selective Determination of Mono- and Dihydroxylated Analogs of Polybrominated Diphenyl Ethers in Marine Sponges by Liquid-Chromatography Tandem Mass Spectrometry. Anal Bioanal Chem 404:197–206. doi:10.1007/s00216-012-6132-2
109. Cotter RJ (1980) Mass Spectrometry of Nonvolatile Compounds by Desorption from Extended Probes. Anal Chem 52:1589A–1602A. doi:10.1021/ac50064a003
110. Kurlansik L, Williams TJ, Strong JM, Anderson LW, Campana JE (1984) Desorption Ionization Mass Spectrometry of Synthetic Porphyrins. Biomed Mass Spectrom 11:475–481. doi:10.1002/bms.1200110908
111. Helleur RJ, Thibault P (1994) Optimization of Pyrolysis-Desorption Chemical Ionization Mass Spectrometry and Tandem Mass Spectrometry of Polysaccharides. Can J Chem 72:345–351. doi:10.1139/v94-053
112. Vincenti M (2001) The Renaissance of Desorption Chemical Ionization Mass Spectrometry: Characterization of Large Involatile Molecules and Nonpolar Polymers. Int J Mass Spectrom 212:505–518. doi:10.1016/S1387-3806(01)00492-4
113. Beuhler RJ, Flanigan E, Greene LJ, Friedman L (1974) Proton Transfer Mass Spectrometry of Peptides. Rapid Heating Technique for Underivatized Peptides Containing Arginine. J Am Chem Soc 96:3990–3999. doi:10.1021/ja00819a043

114. Cullen WR, Eigendorf GK, Pergantis SA (1993) Desorption Chemical Ionization Mass Spectrometry of Arsenic Compounds Present in the Marine and Terrestrial Environment. Rapid Commun Mass Spectrom 7:33–36. doi:10.1002/rcm.1290070108
115. Juo CG, Chen SW, Her GR (1995) Mass Spectrometric Analysis of Additives in Polymer Extracts by Desorption Chemical Ionization and Collisional Induced Dissociation with B/E Linked Scanning. Anal Chim Acta 311:153–164. doi:10.1016/0003-2670(95)00183-Z
116. Chen G, Cooks RG, Jha SK, Green MM (1997) Microstructure of Alkoxy and Alkyl Substituted Isocyanate Copolymers Determined by Desorption Chemical Ionization Mass Spectrometry. Anal Chim Acta 356:149–154. doi:10.1016/S0003-2670(97)00504-7
117. Pergantis SA, Emond CA, Madilao LL, Eigendorf GK (1994) Accurate Mass Measurements of Positive Ions in the Desorption Chemical Ionization Mode. Org Mass Spectrom 29:439–444. doi:10.1002/oms.1210290808
118. Horning EC, Horning MG, Carroll DI, Dzidic I, Stillwell RN (1973) New Picogram Detection System Based on a Mass Spectrometer with an External Ionization Source at Atmospheric Pressure. Anal Chem 45:936–943. doi:10.1021/ac60328a035
119. Horning EC, Carroll DI, Dzidic I, Haegele KD, Horning MG, Stillwell RN (1974) Atmospheric Pressure Ionization (API) Mass Spectrometry. Solvent-Mediated Ionization of Samples Introduced in Solution and in a Liquid Chromatograph Effluent Stream. J Chromatogr Sci 12:725–729. doi:10.1093/chromsci/12.11.725
120. Carroll DI, Dzidic I, Stillwell RN, Horning MG, Horning EC (1974) Subpicogram Detection System for Gas Phase Analysis Based Upon Atmospheric Pressure Ionization (API) Mass Spectrometry. Anal Chem 46:706–704. doi:10.1021/ac60342a009
121. Carroll DI, Dzidic I, Stillwell RN, Haegele KD, Horning EC (1975) Atmospheric Pressure Ionization Mass Spectrometry. Corona Discharge Ion Source for Use in a Liquid Chromatograph-Mass Spectrometer-Computer Analytical System. Anal Chem 47:2369–2373. doi:10.1021/ac60364a031
122. Dzidic I, Stillwell RN, Carroll DI, Horning EC (1976) Comparison of Positive Ions Formed in Nickel-63 and Corona Discharge Ion Sources Using Nitrogen, Argon, Isobutane, Ammonia and Nitric Oxide as Reagents in Atmospheric Pressure Ionization Mass Spectrometry. Anal Chem 48:1763–1768. doi:10.1021/ac50006a035
123. Bruins AP (1991) Mass Spectrometry with Ion Sources Operating at Atmospheric Pressure. Mass Spectrom Rev 10:53–77. doi:10.1002/mas.1280100104
124. Tsuchiya M (1995) Atmospheric Pressure Ion Sources, Physico-Chemical and Analytical Applications. Adv Mass Spectrom 13:333–346
125. Schiewek R, Lorenz M, Giese R, Brockmann K, Benter T, Gaeb S, Schmitz OJ (2008) Development of a Multipurpose Ion Source for LC-MS and GC-API-MS. Anal Bioanal Chem 392:87–96. doi:10.1007/s00216-008-2255-x
126. Warscheid B, Hoffmann T (2001) Structural Elucidation of Monoterpene Oxidation Products by Ion Trap Fragmentation Using on-Line Atmospheric Pressure Chemical Ionization Mass Spectrometry in the Negative Ion Mode. Rapid Commun Mass Spectrom 15:2259–2272. doi:10.1002/rcm.504
127. Derpmann V, Albrecht S, Benter T (2012) The Role of Ion-Bound Cluster Formation in Negative Ion Mass Spectrometry. Rapid Commun Mass Spectrom 26:1923–1933. doi:10.1002/rcm.6303
128. Klee S, Derpmann V, Wissdorf W, Klopotowski S, Kersten H, Brockmann KJ, Benter T, Albrecht S, Bruins AP, Dousty F, Kauppila TJ, Kostiainen R, O'Brien R, Robb DB, Syage JA (2014) Are Clusters Important in Understanding the Mechanisms in Atmospheric Pressure Ionization? Part 1: Reagent Ion Generation and Chemical Control of Ion Populations. J Am Soc Mass Spectrom 25:1310–1321. doi:10.1007/s13361-014-0891-2
129. McEwen CN, Larsen BS (2009) Ionization Mechanisms Related to Negative Ion APPI, APCI, and DART. J Am Soc Mass Spectrom 20:1518–1521. doi:10.1016/j.jasms.2009.04.010

130. Hayen H, Karst U (2003) Strategies for the Liquid Chromatographic-Mass Spectrometric Analysis of Non-Polar Compounds. J Chromatogr A 1000:549–565. doi:10.1016/S0021-9673(03)00505-3
131. Mottram H, Woodbury SE, Evershed RP (1997) Identification of Triacylglycerol Positional Isomers Present in Vegetable Oils by High Performance Liquid Chromatography/Atmospheric Pressure Chemical Ionization Mass Spectrometry. Rapid Commun Mass Spectrom 11:1240–1252. doi:10.1002/(SICI)1097-0231(199708)11:12<1240::AID-RCM990>3.0.CO;2-5
132. Reemtsma T (2003) Liquid Chromatography-Mass Spectrometry and Strategies for Trace-Level Analysis of Polar Organic Pollutants. J Chromatogr A 1000:477–501. doi:10.1016/S0021-9673(03)00507-7
133. Covey TR, Thomson BA, Schneider BB (2009) Atmospheric Pressure Ion Sources. Mass Spectrom Rev 28:870–897. doi:10.1002/mas.20246
134. Hayen H, Jachmann N, Vogel M, Karst U (2003) LC-Electron Capture-APCI(-)-MS Determination of Nitrobenzoxadiazole Derivatives. Analyst 128:1365–1372. doi:10.1039/B308752B
135. Hayen H, Jachmann N, Vogel M, Karst U (2002) LC-Electron Capture APCI-MS for the Determination of Nitroaromatic Compounds. Analyst 127:1027–1030. doi:10.1039/B205477A
136. Robb DB, Covey TR, Bruins AP (2000) Atmospheric Pressure Photoionization: an Ionization Method for Liquid Chromatography-Mass Spectrometry. Anal Chem 72:3653–3659. doi:10.1021/ac0001636
137. Keski-Hynnilä H, Kurkela M, Elovaara E, Antonio L, Magdalou J, Luukkanen L, Taskinen J, Koistiainen R (2002) Comparison of Electrospray, Atmospheric Pressure Chemical Ionization, and Atmospheric Pressure Photoionization in the Identification of Apomorphine, Dobutamine, and Entacapone Phase II Metabolites in Biological Samples. Anal Chem 74:3449–3457. doi:10.1021/ac011239g
138. Syage JA, Hanold KA, Lynn TC, Horner JA, Thakur RA (2004) Atmospheric Pressure Photoionization. II Dual Source Ionization. J Chromatogr A 1050:137–149. doi:10.1016/j.chroma.2004.08.033
139. Yang C, Henion JD (2002) Atmospheric Pressure Photoionization Liquid Chromatographic-Mass Spectrometric Determination of Idoxifene and Its Metabolites in Human Plasma. J Chromatogr A 970:155–165. doi:10.1016/S0021-9673(02)00882-8
140. Kauppila TJ, Kuuranne T, Meurer EC, Eberlin MN, Kotiaho T, Koistiainen R (2002) Atmospheric Pressure Photoionization Mass Spectrometry. Ionization Mechanism and the Effect of Solvent on the Ionization of Naphthalenes. Anal Chem 74:5470–5479. doi:10.1021/ac025659x
141. Raffaeli A, Saba A (2003) Atmospheric Pressure Photoionization Mass Spectrometry. Mass Spectrom Rev 22:318–331. doi:10.1002/mas.10060
142. Kauppila TJ, Syage JA, Benter T (2015) Recent Developments in Atmospheric Pressure Photoionization-Mass Spectrometry. Mass Spectrom Rev XX:1–27. doi:10.1002/mas.21477
143. Kauppila TJ, Kostiainen R, Bruins AP (2004) Anisole, a New Dopant for Atmospheric Pressure Photoionization Mass Spectrometry of Low Proton Affinity, Low Ionization Energy Compounds. Rapid Commun Mass Spectrom 18:808–815. doi:10.1002/rcm.1408
144. Robb DB, Covey TR, Bruins AP (2001) Atmospheric Pressure Photoionization (APPI): A New Ionization Technique for LC/MS. Adv Mass Spectrom 15:391–392
145. Kauppila TJ, Kersten H, Benter T (2014) The Ionization Mechanisms in Direct and Dopant-Assisted Atmospheric Pressure Photoionization and Atmospheric Pressure Laser Ionization. J Am Soc Mass Spectrom 25:1870–1881. doi:10.1007/s13361-014-0988-7
146. Ahmed A, Choi CH, Kim S (2015) Mechanistic Study on Lowering the Sensitivity of Positive Atmospheric Pressure Photoionization Mass Spectrometric Analyses: Size-Dependent Reactivity of Solvent Clusters. Rapid Commun Mass Spectrom 29:2095–2101. doi:10.1002/rcm.7373

147. Kauppila TJ, Kotiaho T, Kostiainen R, Bruins AP (2004) Negative Ion-Atmospheric Pressure Photoionization-Mass Spectrometry. J Am Soc Mass Spectrom 15:203–211. doi:10.1016/j.jasms.2003.10.012
148. Sioud S, Kharbatia N, Amad MH, Zhu Z, Cabanetos C, Lesimple A, Beaujuge P (2014) The Formation of [M-H]+ Ions in *n*-Alkyl-Substituted Thieno[3,4-*c*]-Pyrrole-4,6-Dione Derivatives During Atmospheric Pressure Photoionization Mass Spectrometry. Rapid Commun Mass Spectrom 28:2389–2397. doi:10.1002/rcm.7031
149. Fredenhagen A, Kuehnoel J (2014) Evaluation of the Optimization Space for Atmospheric Pressure Photoionization (APPI) in Comparison with APCI. J Mass Spectrom 49:727–736. doi:10.1002/jms.3401